[S-7]

Role of Toxicogenomics Technology as a Future Tool for Toxicity Evaluation

Joon-Suk Park, Jae-Woong Hwang, Yong-Soon Lee and Kyung-Sun Kang

Department of Veterinary Public Health, College of Veterinary Medicine,
Seoul National University, Seoul, Korea

Studies in toxicology measure the effects of an agent on an organism' food consumption and digestion, on its body and organ weight, on microscopic histopathology, and cell viability, immortalization, necrosis and apoptosis. The rapid accumulation of genomic-sequence data and associated gene and protein annotation has promoted the application of gene-expression analysis to understanding toxic mechanism of chemicals and other environmental stressors on biological systems. Toxicogenomics allow the toxicologist to investigate the relationship to thousands of gene products or small molecules to toxic mechanism. Toxicogenomics is expected to provide data that may much of the present uncertainty in extrapolating from laboratory animal models to the human situation. Toxicogenomics could be incorporated into routinely applied existing regulatory tests to retrieve mechanistic information in addition to conventional toxicity endpoints. Furthermore, toxicogenomics will contribute to the discovery of new biomarkers of human exposure. Using toxicogenomic markers of exposure, the internal exposure could be detected individually. Additionally, markers of effects and susceptibility could be used which overall would enable a more effective utilization of epidemiological study.

Molecular mechanisms of the 2,3,7,8-tetrachlorodibenzo-p-dioxin-induced inverted U-shaped dose responsiveness in anchorage independent growth and cell proliferation of human breast epithelial cells with stem cell characteristics

Nam-Shik Ahn [a,1], Hongbo Hu [a,1], Jin-Sung Park [a], Joon-Suk Park [a],
Jong-Sik Kim [b], Sungwhan An [b], Gu Kong [c], Okezie I. Aruoma [a,d],
Yong-Soon Lee [a], Kyung-Sun Kang [a,*]

[a] Laboratory of Stem Cell and Tumor Biology, Department of Veterinary Public Health, College of Veterinary Medicine, Seoul National University, San 56-1 Sillim-Dong, Kwanak-Gu, Seoul 151-742, Republic of Korea
[b] Microarray Division, GenomicTree, Inc., Jonmin-Dong 461-6, Yusong-Gu, Daejon 305-390, Republic of Korea
[c] Department of Pathology, College of Medicine and Molecular Biomarker Research Center, Hanyang University, Seoul 133-791, Republic of Korea
[d] Faculty of Health and Social Care, London South Bank University, 103 Borough Road, London SE1 0AA, UK

Received 7 February 2005; received in revised form 2 March 2005; accepted 7 March 2005

Abstract

Although 2,3,7,8-tetrachlorodibenzo-p-dioxin (TCDD) has a variety of carcinogenic and noncarcinogenic effects in experimental animals, its role in human carcinogenicity remain controversial. A simian virus 40-immortalized cell line from normal human breast epithelial cells with stem cells and luminal characteristics (M13SV1) was used to study whether TCDD can induce AIG positive colony formation and cause increased cell numbers in a inverted U-shaped dose–response manner. TCDD activated Akt, ERK2, and increased the expression of CYP1A1, PAI-2, IL-lb mRNA, and ERK2 protein levels. TCDD was able to increased phosphorylation and expression of ERK2 in same dose–response manner as AIG positive colony formation. Thus, TCDD induced tumorigenicity in M13SV1, possibly through the phosphorylation of ERK2 and/or Akt. Further, cDNA microarray with 7448 sequence-verified clones was used to profile various gene expression patterns after treatment of TCDD. Three clear patterns could be delineated: genes that were dose-dependently up-regulated, genes expressed in either U-shape

* Corresponding author. Tel.: +82 2 880 1246; fax: +82 2 876 7610.
  E-mail address: kangpub@snu.ac.kr (K.-S. Kang).
[1] Authors contributed equally to this work.

and/or inverted U-shape. The fact that these genes are intrinsically related to breast epithelial cell proliferation and survival clearly suggests that they may be involved in the TCDD-induced breast tumorigenesis.

1. Introduction

The International Agency for Cancer Researh on Cancer (IARC) have classified 2,3,7,8-tetra-chlorodibenzo-*p*-dioxin (TCDD) as a human carcinogen. TCDD is a prototype and the most potent chemical of the polychlorinated dibenzo-*p*-dioxins and polychlorinated dibenzofurans (dioxins). A animal exposure to TCDD can result in various adverse effects which includes carcinogenesis, endometriosis, and immunotoxicicty [1–3]. Developmental neurobe-havioral (cognitive) dysfunctions and developmental reproductive (reduction of sperm number, female urogenital malformations) abnormalities are widely reported [4–6]. However, there is an ongoing debate as to the human carcinogenic potentials of the exposure to dioxin [7,8]. Thus, it is important to assess the molecular mechanisms that could mitigate the car-cinogenic potentials of TCDD in humans making use of the immortalized human breast epithelial cell line (MCF-10A), human keratinocyte cell line (HaCaT) and endometrial cell line. Immortalized human cell systems have both infinite life span and normal human cell characteristics. Immortalized human cell systems continue to be suggested for use in the screening human carcinogens as well as in the study of their molecular mechanisms [9–12]. As such, these groups of cells may not only facilitate detection of carcinogenicity but provide valuable insights into the carcinogenic process in humans. Our laboratory have established normal human breast stem cells from reduction mammoplasty and human breast immortalized cell line, namely M13SV1, simian virus 40-immortalized cell line from normal human breast epithelial cells with stem cells and luminal characteristics [13,14]. These cells were used to examine MHC expression in a human adult stem cell line and its down-regulation by hCMV US gene transfection [15]. The ability of TCDD to induce tumorigenicity in these non-tumorigenic immortalized human breast epithelial cells was assessed. Indeed TCDD was able to induce anchorage-independent

growth (AIG) positive colony formation in M13SV1 cells in an inverted U-shaped dose–response manner, and which correlates with its ability to increase cell number. Further, TCDD was found to increase the expression of CYP1A1, PAI-2, IL-1 mRNA, and ERK2 protein as well as activating Akt and ERK2. More importantly, TCDD increased the phosphorylation and expression of ERK2 in same dose–response manner as AIG positive colony formation.

2. Materials and methods

2.1. Chemicals and reagents

TCDD was purchased from GL Sciences, Inc. (Tokyo, Japan). Rabbit polyclonal Akt and phospho-Akt antibodies were purchased from Cell Signaling Technology. Rabbit polyclonal MAP kinase antibody was purchased from Zymed Laboratories, Inc. (South San Francisco, CA, USA). Rabbit polyclonal phospho-MAP kinase and phospho-p38 kinase antibodies were purchased from Promega Corporation (Medison, WI, USA). Mouse monoclonal p38 kinase, rabbit poly-clonal JNK1 and mouse monoclonal phospho-JNK1 antibodies were purchased from Santa Cruz Biotech-nology, Inc. (Santa Cruz, CA, USA). FBS was from Gibco Laboratory (Carlsbad, CA, USA).

2.2. Cell culture

The immortalized human breast luminal epithe-lial cell line (M13SV1) generated by transfection of Type I normal human breast epithelial cells (HBEC) from women undergoing reduction mammoplasty with SV40 DNA in a previous study [13] was used. M13SV1 cells were cultured as previously described [14]. Early passage cells were thawed from liquid nitrogen storage and were cultured in MSU-1 medium containing 10% fetal bovine serum (FBS). Cultures were maintained in a 5% CO^2/95% humidified air at 37 °C.

2.3. Cell proliferation assay

The effect of TCDD on cell proliferation was measured by direct cell counting. Ml3SVl cells (3×10^4 cells) were plated at 100-mm cell culture dish. The cells were then treated with various concentrations of TCDD (0.01, 0.1, 1, 10, 100 nM dissolved in DMSO) or vehicle, DMSO (0.1%), as negative control for 7, 14, and 21 days. The effect of TCDD on cell proliferation was measured by direct cell counting with cell counting chamber. At least three independent experiments were performed for each study.

2.4. Anchorage-independent growth assay

Anchorage-independent growth (AIG) capability was determined by assessing the colony-forming efficiency of cells suspended in soft agar. Agarose (0.5% Type I, Low EEO; Sigma Chemical Co.) prepared in MSU-1 medium at 39 °C was added to 60-mm dishes and allowed to solidify in the incubator. M13SV1 (1×10^4) suspended in mediun with 0.33% agarose were overlaid on top of hard layer 0.5% agar. After 1 day, the cells were treated with various concentrations of TCDD. The medium containing TCDD was renewed every 3 days. At the end of 2 weeks, the medium was removed and colonies of cells were stained with 1 mg/ml tetrazolium salt (Sigma Chemical Co., USA). Colonies ≥ 0.25 mm were counted using an inverted phase microscope and calibrated template.

2.5. cDNA microarray preparation

A set of 7448 sequence-verified human cDNA clones was purchased from Research Genetics, Inc. (Huntsville, AL, USA). Bacterial clones were amplified in 96-well culture plates. Plasmid DNA was isolated using a Millipore plasmid kit (Millipore, Bedford, MA, USA) and ORFs were PCR-amplified using a pair of universal primers, 5′-CTGCAAGGC-GATTAAGTTGGGTAAC-3′ and 5′-GTGAGCGGA-TAACAATTTC-ACACAGGAAACAGC-3′ under the following conditions: initial denaturation at 94 °C for 2 min, followed by 30 cycles of 94 °C for 45 s, 55 °C for 45 s, and 72 °C for 2 min, and a final extension step at 72 °C for 10 min. The PCR amplification products were examined by 1% agarose gel electrophoresis, purified using a Sephadex G-50 column, dried and then resus-pended in a 50% DMSO solution. DNA was spotted by an OmniGrid™ Microarrayer (GeneMachines, Inc., San Carlos, CA, USA) onto a silanized glass slide surface (CMT-GAPS™, Corning, Charlotte, NC, USA). Each slide was crosslinked with 300 mJ short wave UV irradiation (Stratalinker, Stratagene, La Jolla, CA, USA) and stored in a desiccator [14].

2.6. Total RNA isolation, probe preparation, and hybridization

M13SV1 cells were plated in 75 cm² tissue culture flask (Nunc) in triplicate and allowed to attached for 24 h. The cells were treated with various concentrations of TCDD or its vehicle, DMSO (0.1%), as negative control for 2 weeks. Total cellular RNA was extracted from the cells by using TRIzol Reagent™ (Invitrogen, Carlsbad, CA) according to the manufacturer's instructions. The extracted RNA was dissolved in RNase-free water, and its concentration and purity was determined from absorbance measurements at 260 and 280 nm using a spectrophotometer. Quality of the RNA was checked by visualizaion of the 28S:18S ribosomal RNA ratio on a 1% agarose gel. The overall procedure of hybridization was performed according to Dr. Patrick O'Brown's laboratory protocol (http://cmgm.stanford.edu/pbrown). Briefly, 100 μg each of total RNA from vehicle-treated or TCDD-treated cells was reverse-transcribed using oligo-dT primers (5′-TTTTTTTTTTTTTTTTTTTTTTVN-3′) in the presence Cy3-dUTP or Cy5-dUTP, respectively. The labeled cDNA probe was then purified through a microcon-30 column. The purified probe was next resuspended in 80 μl of hybridization solution (3× SSC and 0.3% SDS). The probe was then denatured at 100 °C for 2 min and applied to the DNA chip at 65 °C for 16 h in a humidified chamber. Finally, the hybridized slide was washed once each in 2× SSC for 2 min, 0.1× SSC, 0.1% SDS for 5 min, and 0.1× SSC for 5 min and then spun-dried prior to scanning at room temperature.

2.7. Data acquisition and analysis

Fluorescent cDNA probes hybridized to a cDNA microarray were detected by scanning the slide with a GenePix 4000B scanner (Axon instruments, Foster City, CA, USA). The scanned image was then ana-

lyzed using the GenePix Pro 3.0 software package. Signal intensity values were determined by subtracting the background median value from the intensity median value of each spot. Expression values were normalized by a single multiplicative normalization factor and applied to all Cy5/Cy3 ratios so that the median normalized Cy5/Cy3 ratio became 1.0. The relationship between the gene expression profile and TCDD treatment in terms of log ratios was calculated by applying the 'average-linkage hierarchical clustering' method in a CLUSTER program. The result was visualized with the TREEVIEW program (available at http://www.microarrays.org).

2.8. Reverse transcription-polymerase chain reaction (RT-PCR) analysis

Total RNA was extracted with Trizol reagent (Gibco Laboratory, Calsbad, CA, USA) according to the method described by the manufacturer, and then RNA extract was stored at −80 °C until use. The cDNAs for RT-PCR analysis were synthesized from 5 μg of total RNA in a 30-μl reaction mixture as described by the manufacturer (Gibco Laboratory, USA) and a PCR was performed using Touchdown temperature cycling system (Hybaid, UK). GAPDH served as an internal control. Primers used for cytochrome P450 1 Al were CYP1A1 forward (5′-AACCAC-GTTGCAGGAGCTGAT-3′) and reverse (5′-ACAT-TGGCGTTCTCATCCAGCTGCT-3′) for amplification of a 387-bp fragment of CYP1A1 cDNA; for PAI-2, forward (5′-TTCATCCTTCCGCTCTCTCAG-3′), reverse (5′-CTTCAGTGCCCTCCTCATTCA′-3) for amplification 794-bp fragment of PAI-2 cDNA; for IL-lb, forward (5′-AAACAGATGAAGTGCTCC-TTCCAGG-3′), reverse (5′-TGGAGAACACCACT-TGTTCTCCA-3′) for amplification 388-bp fragment of IL-lb cDNA; for ITGA5, forward (5′-AA-CCACGTTGCAGGAGCTGAT-3′), reverse (5′-AC-ATTGGCGTTCTCATCCAGCTGCT-3′) for amplification 137-bp fragment of ITGA5 cDNA; for TSP1, forward (5′-TTCATCCTTCCGCTCTCTCAG-3′), reverse (5′-CTTCAGTGCCCTCCTCATTCA-3′) for amplification 331-bp fragment of TSP1 cDNA; CYBA, forward (5′-AAACAGATGAAGTGCTCCT-TCCAGG-3′), reverse (5′-TGGAGAACACCACTT-GTTCTCCA-3′) for amplification 118-bp fragment of CYBA; for GAPDH, forward (5′-CGGAGTCA-

ACGGATTTGGTCGTAT-3′), reverse (5′-AGCCTT-CTCCATGGTGGTGAAGAC-3′) for amplification 306-bp fragment of GAPDH cDNA. After an initial denaturing step at 95 °C for 10 min, amplification for the CYP1A1 mRNA and GAPDH mRNA was performed with 30 cycles at 95 °C for 1 min, 60 °C for 1 min, 72 °C for 1.5 min, and further extension for 10 min. For the PAI-2 mRNA and IL-1b mRNA, 40 cycles at 95 °C for 1 min, 61 °C (PAI-2) or 58 °C (IL-1b) for 1 min, 72 °C for 1.5 min, and further extension at 72 °C for 10 min were performed. For ITGA5 mRNA, 25 cycles at 95 °C for 1 min, 55 °C for 1 min, 72 °C for 1.5 min, and further extension at 72 °C for 10 min were performed. For TSP1 mRNA and CYBA mRNA, 30 cycles at 95 °C for 1 min, 55 °C for 1 min, 72 °C for 1.5 min, and further extension at 72 °C for 10 min were performed. PCR products were analyzed by electrophoresis through 1.5% agarose gels containing 0.1 mg/ml of ethidium bromide. Images of the RT-PCR ethidium bromide-stained agarose gels were acquired with UV illumination on a GelDoc2000/ChemiDoc System (Bio-Rad) and quantification of the bands was performed by densitometry using the Quantity One software (version 4.0.1; Bio-Rad).

2.9. Western blot analysis

Assays of ERKs, p38 kinase, JNKs, and Akt were carried out as described in the protocol provided by manufacturers. The M13SV1 cells were grown in a 100-mm cell culture dish, and when cell density reached 80–90% confluence, cells were treated with various concentrations of TCDD or its vehicle, DMSO (0.1%), as negative control for 6, 12, and 24 h, respectively. In a 2 weeks protocol, 10,000 cells were plated in each 100-mm dish. After 1 day, the cells were treated with various concentrations of TCDD or its vehicle, DMSO (0.1%), as negative control for 2 weeks. The cells were then washed with ice-cold PBS and lysed with lysis buffer (20% SDS containing 2 mM phenymethylsulfonyl fluoride, 10 mM iodoacetoamide, 1 mM leupeptin, 1 mM antipain, 0.1 mM sodium orthovanadate and 5 mM sodium fluoride) for 10 min. The lysates were sonicated three times at 10-s intervals, aliquoted and stored at −20 °C. The protein concentration was determined by the Bio-Rad DC protein assay (Bio-Rad Laboratories, Hercules, CA, USA). Equal amounts of protein (20 μg/lane) were subjected

to 12% SDS-PAGE and transferred to nitrocellulose membranes. Membranes were probed with phosphorylated and total ERKs, p38, JNKs and Akt antibodies, respectively, followed by incubation with horseradish peroxidase-conjugated secondary antibody. Antibody-bound proteins were detected by the ECL Western blotting analysis system (Amersham Pharmacia Biotech Limited, UK).

3. Results

3.1. TCDD increases M13SV1 cell number and induces AIG positive colony formation in an inverted U-shaped dose–response manner

M13SV1 cells were treated with various non-toxic concentrations of TCDD or 0.1% DMSO for 7, 14 or 21 days in normal growth conditions. TCDD significantly increased cell number compared with vehicle control in an inverted U-shaped dose–response manner (Fig. 1A). A 1 nM concentration of TCDD increased cell number by almost 3-fold and this declined with increasing concentrations of TCDD (Fig. 1A and C). These results suggest that TCDD was capable of up-regulating normal cell growth in normal growth conditions which indicates a relationship to tumorigenic potentials. In the AIG assay, TCDD was able to induce AIG positive colony formation in M13SV1 cell in the same dose–response manner (Fig. 1B and C). Again, the 1 nM TCDD was effective in increasing the cell numbers.

3.2. TCDD increases expression of CYP1A1, PAI-2, and IL-1β mRNA in a dose–response manner

Many of endocrine disrupting chemicals show inverted U-shaped dose–response curve. TCDD is also an endocrine disruptor. So RT-PCR assay was used to assess the possibility of the inverted U-shape of dose–response being induced by TCDD. Among dioxin-responsive genes, the regulation of CYP1A1 gene expression is the most studied and well established. The PAI-2, and IL-1β genes are also expressed dose-dependently in keratinocytes, and endometrial cells following exposure to TCDD. The expression of CYP1A1, PAI-2, and IL-1β mRNA were analyzed by
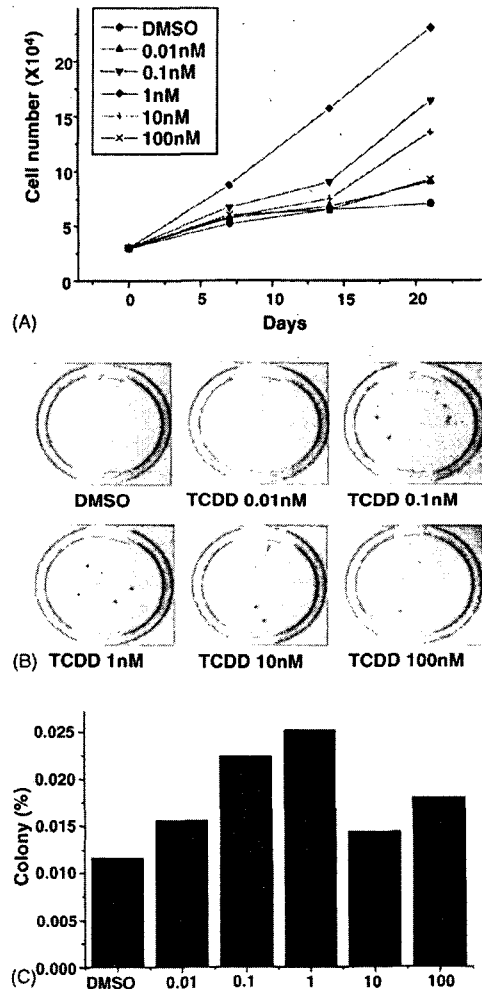
Fig. 1. Effect of TCDD on the cell growth of M13SV1 non-tumorigenic human breast luminal epithelial cells. (A) Cell growth curve assay. M13SV1 were seeded and incubated for 7, 14, and 21 days. The cells were then treated with various concentrations of TCDD (0.01, 0.1, 1, 10, 100 nM dissolved in DMSO) or vehicle, DMSO (0.1%), as negative control. Data are the mean of at least three different experiments. (B and C) Soft agar assay with M13SV1 cells. The cells were then treated with various concentrations of TCDD or DMSO (0.1%). After 2 weeks, colonies of cells were stained with tetrazolium salt. Colonies ≥ 0.25 mm were counted.

CYP1A1 (387bp)

GAPDH (306bp)

PAI-2 (794bp)

GAPDH (306bp)

IL-1β (388bp)

GAPDH (306bp)

(A) DMSO T0.01 T0.1 T1 T10 T100

(B) DMSO T0.01 T0.1 T1 T10 T100

(C) DMSO T0.01 T0.1 T1 T10 T100

Fig. 2. Results of RT-PCR after the exposure to various concentrations of TCDD. (A) Cytochrome P450 1A1; (B) plasminogen activator inhibitor 2; (C) interleukin 1β.

0.01nM 0.1nM 1nM 10nM 100nM

B-factor. properdin
lipocalin 2 (oncogene 24p3)
myxovirus (influenza) resistance 1. homo
interferon. alpha-inducible protein (clo
major histocompatibility complex. class
laminin receptor 1 (67kD. ribosomal prot
major histocompatibility complex, class
2'-5'oligoadenylate synthetase 3
fibulin 1
epithelial membrane protein 2
guanine nucleotide binding protein (G pr
alanyl (membrane) aminopeptidase (amino
integrin. alpha 5 (fibronectin receptor.
small glutamine-rich tetratricopeptide r
cytochrome b-245. alpha polypeptide
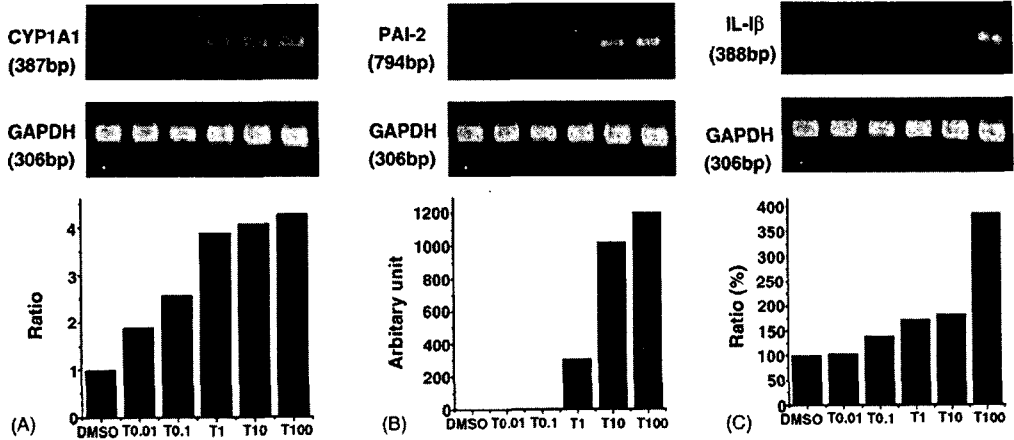melanoma adhesion molecule
melanoma adhesion molecule
U5 snRNP-specific protein (220 kD). orth
SHC (Src homology 2 domain-containing) t
-
-
-
ubiquinol-cytochrome c reductase hinge p
thrombospondin 1
ring finger protein 10
mevalonate (diphospho) decarboxylase
PPAR(gamma) angiopoietin related protein
adipose differentiation-related protein:
adipose differentiation-related protein:
cytochrome P450, subfamily I (dioxin-ind
epiregulin

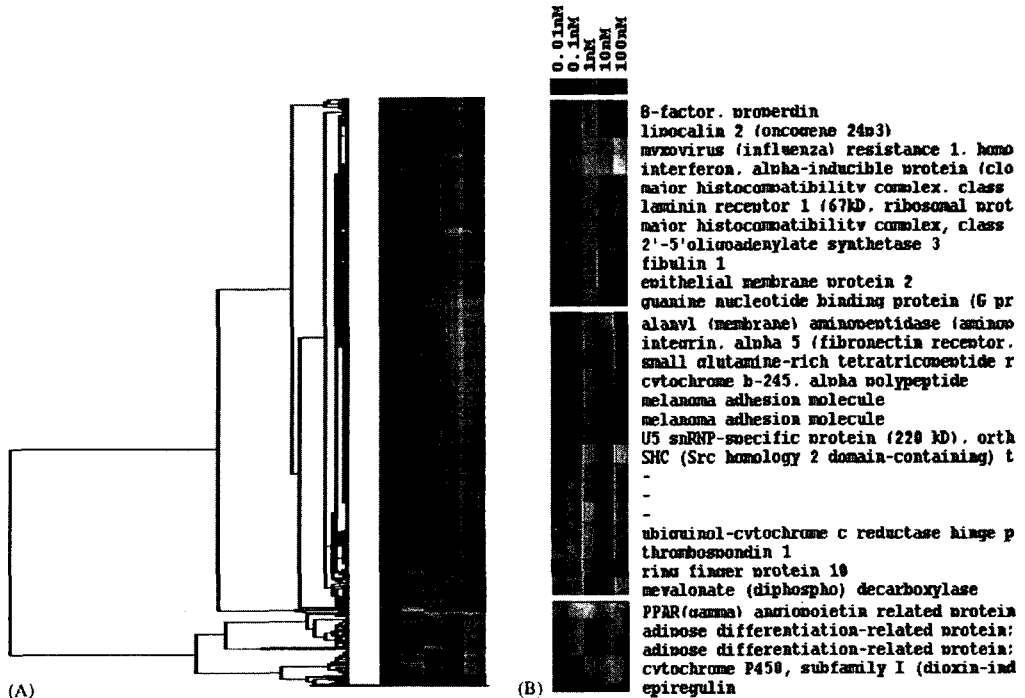(A)   (B)

Fig. 3. Clustering analysis on gene expression profiles of TCDD-treated M13SV1 cells. (A) cDNA microarray analysis was done to evaluate gene expression changes in response to TCDD treatment. (B) Following 2-week treatment, induced expression profiles in various concentrations of TCDD or DMSO were found to classify into three interesting group related to TCDD-induced tumorigenesis.

RT-PCR and as shown in Fig. 2, TCDD was able to increase the expression of CYP1A1, PAI-2, and IL-1β in a dose–response manner.

3.3. Profiling of genes, which related with TCDD-induced tumorigenicity in M13SV1, by cDNA microarray analysis

The genes that are up- or down-regulated over 2-fold in the 1 nM TCDD-treated group were assessed. Of the genes, 19 were up-regulated and 8 genes were down-regulated by 2-fold or more (Fig. 3). In order to establish which of the genes are related to TCDD-induced tumorigenesis, those genes were further classified: dose-dependently up-regulated genes, genes expressed in either U-shape and/or inverted U-shape. The dose-dependently up-regulated genes were composed of angiopoietin-like 4, adipose differentiation-related protein, cytochrome P450, subfamily I (dioxin-inducible), and epiregulin. The genes that were expressed in the U-shape pattern contained B-factor, lipocalin 2, interferon, alpha-inducible protein, major histocompatibility complex, class I, C, and major histocompatibility complex, class I. Finally, those genes expressed in inverted U-shape were composed of ring finger protein 10 (RNF10), thrombospodin 1 (TSP1), integrin alpha 5 (ITGA5), melanoma cell adhesion molecule (MCAM), eukaryotic translation initiation factor 4 gamma 1 (EIF4G1), pre-mRNA processing factor 8 homolog (PRP8) and Src homology 2 domain containing (SHC) transforming protein 1 (Fig. 3). Semi-quantitative RT-PCR analysis was performed for the three chosen genes integrin alpha 5, thrombospodin; cytochrome *b*-245 (CYBA) in order to verify the identity of these genes and to set the reliability of the microarray data. RT-PCR was executed to verify the data of microarray (Fig. 4). These results indicate that a qualitative correlation existed between RT-PCR and the microarray data.

3.4. TCDD activates Akt, ERK2, and increases expression of ERK2, but not ERK1, p38 and JNK1

The signaling pathways underlying TCDD-induced AIG positive colony formation in M13SV1 cells were assessed using Western blot analysis of Akt, ERKs, p38, and JNK1. TCDD induced prolonged Akt activation starting at 6 h in an inverted U-shaped dose

dependent manner, at 12 h in a dose dependent manner and 2 weeks after treatment in an inverted U-shaped manner again (Fig. 5A). Levels of total Akt were unchanged (Fig. 5A). Compared with prolonged activation of Akt, TCDD induced early and transient activation of ERK2, but not ERK1 at 6 h (but this was not detectable by 12 h) after treatment in an inverted U-shaped dose–response manner (Fig. 5B), which paralleled the manner of AIG positive colony formation. Whereas levels of total ERK2, but not ERK1 were increased starting 24 h and continuing through 2 weeks after treatment with TCDD in same manner as activation of ERK2 (Fig. 5B). TCDD treatment neither activated p38 and JNK1, nor changed p38 and JNK1 (Fig. 5B), suggesting that TCDD induce AIG positive colony formation in M13SV1 cell line possibly through the phosphorylation of Akt and/or ERK2.

4. Discussion

Molecular studies have shown that TCDD prevents apoptosis in the human breast epithelial cell line (MCF-10A), and that AKT and ERK phosphorylation correlates with inhibition of apoptosis [16]. TCDD is also able to act as a rodent tumor promoter by inhibiting apoptosis in initiated liver [17,18]. The ability of TCDD to alter cell growth in M13SV1 cells was assessed with the working hypothesis that TCDD could increase cell numbers by inhibiting apoptosis, and that the TCDD-induced cell number increase could be related to tumorigenicity. Indeed TCDD induced cell number increase and anchorage-independent cell growth in M13SV1 cell line. Interestingly, low dose TCDD-treated group enhanced cell growth but not at the higher doses resulting in an inverted U-shaped dose–response manners (Fig. 1).

A cDNA microarray probe containing 7.5 K genes representing broad cellular functions, including oncogenes, tumor suppressor genes and genes involved in cell cycle control, cell–cell interactions, apoptosis as well as signal transduction pathways was used to assess the effect of TCDD on gene induction. Given that cell proliferation and AIG assays can be used to demonstrate inverted U-shaped dose–response, genes that expressed dose–response U-shaped manner or inverted U-shaped manner were assessed by the methods. Myxovirus resistance 1 (interferon-inducible protein p78,
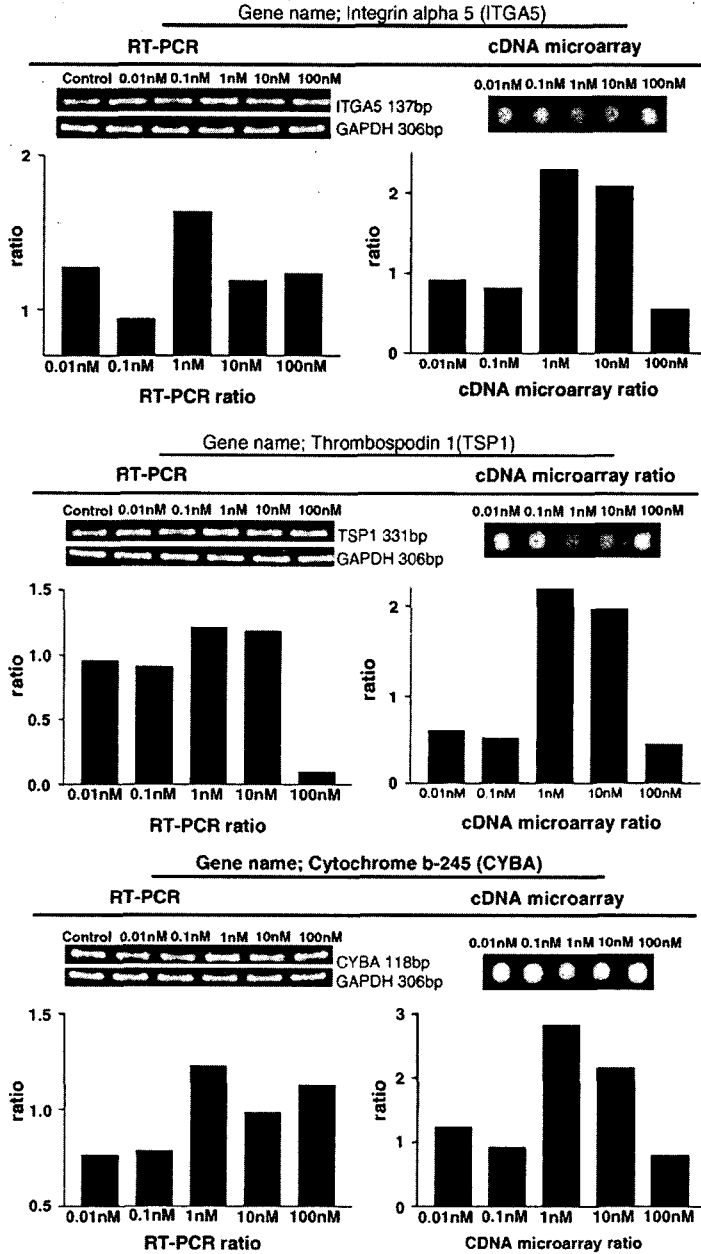
Fig. 4. Confirmation by RT-PCR of microarray results using RNA in TCDD-treated M13SV1 cells. ITGA5, TSP1, CYBA, and GAPDH were amplified and products were seperated in a 1.5% agarose gel and stained with ethidiun bromide. GAPDH was used as the control for equivalent, RNA template among the five samples in the PCR reactions. The RT-PCR experiments were repeated at least twice.
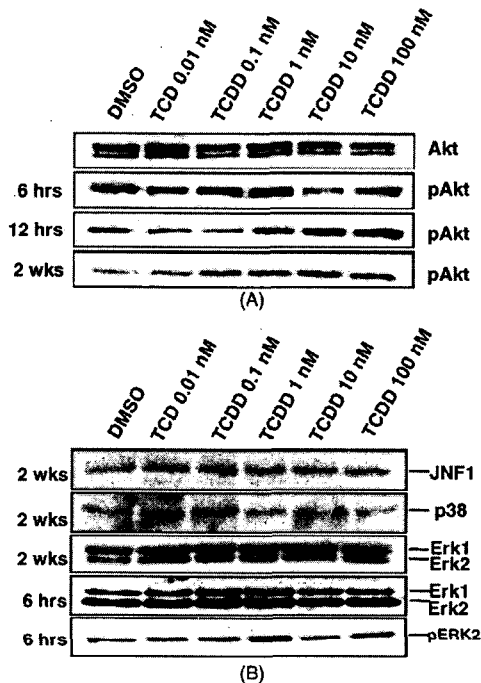
Fig. 5. Akt, ERKs, p38, JNK1 expression after treatment with TCDD using Western blot analysis. (A) Akt expression and (B) JNK1, ERK, p38 expression.

MX 1), major histocompatibility complex (class I, C, HLA-C), major histocompatibility complex (class I, B, HLA-B), 2′,5′-oligoadenylate synthetase 3 (100 kDa, OSA3), and B-Factor (properdin, BF) are genes related to immune system, which were shown U-shaped dose-dependent expression pattern. The immune system is one of its most sensitive target for TCDD toxicity [19,20]. The suppression of immune response will not only leave an organ or tissue susceptible to infections but also to neoplasms as shown by the association of immune deficiencies with Kaposi's sarcoma [21], non-Hodgkin's lymphoma [22] and anogenital carcinoma [23]. Melanoma adhesion molecule (MCAM, MUC18, CD146) and eukaryotic translation initiation factor 4 gamma 1 (EIF4G1), shown U-shaped dose-dependent expression pattern, are known as progression marker in melanoma [24], and gene over-expressed in lung carcinoma [25] and NIH3T3 cell [26], respectively. Integrin alpha5 and thrombospondin-1 were known cell adhe-sion molecules, which were shown U-shaped dose-dependent expression pattern. Generally, cell adhesion molecules play a role in angiogenesis [27,28], and metastasis of cancer [29,30]. Ring finger protein 10 (RNF10, known as adaptor protein in transcription regulation), Src homology 2 domain-containing trans-forming protein 1 (SHC1, known as related to protein tyrosine kinase) showed inverted U-shaped expression patterns whilst fibulin 1 (FBLN1, known as genes reducing phosphorylation of ERK) showed U-shaped expression patterns. These genes were associated with intracellular signal pathways. These genes are closely related to tumor and cancer [31,32] data presented here supported the assertion that TCDD was tumorigenic in M13SV1 cells.

The inhibition of apoptosis by growth factor signal-ing pathway is one possible mechanism of tumor pro-motion/progression [33,34]. It is reasonable to expect the TCDD-induced tumorigenecity to involve alter-ations in cell signaling. To this end, the integrity of the mitogen-activating protein kinase (MAPK) cas-cades was assessed by Western blot analysis. MAPK cascades transmit and amplify signals involved in cell proliferation as well as cell death, and ERK is most relevant to breast cancer [35]. TCDD treat-ment neither activated p38, JNK1, and ERK1, nor changed p38, JNK, and ERK1 protein levels, but activated ERK2, and activated ERK2 protein level, increased in inverted U-shaped dose–response man-ner. The serine/threonine kinase Akt plays a criti-cal role in the growth factor-mediated survival of cells by phosphorylating and thus deactivating com-ponents of the apoptotic machinery such as BAD and caspase-9 [36]. Here, The AKT protein level was not changed, but activated AKT protein level was changed in an inverted U-shaped dose–response manner. Thus, TCDD-induced tumorigenicity clearly involved the ERK and AKT pathway in human breast cancer epithe-lial cells.

In summary, cell proliferation assay and AIG assay show that TCDD could induce tumorigenicity in M13SV1. The Western blot and genomic approaches reveal alterations in the expression profile of genes associated with tumorigenicity in human breast epithe-lial cell line (M13SV1), which involves the ERK2 and AKT pathways. Thus, the activation of these signal transduction pathways was associated with TCDD-induced tumorigenicity.

Acknowledgements

References

[1] M. Viluksela, Y. Bager, J.T. Tuomisto, G. Scheu, M. Unkila, R. Pohjanvirta, S. Flodstrom, V.M. Kosma, J. Maki-Paakkanen, T. Vartiainen, C. Klimm, K.W. Schramm, L. Warngard, J. Tuomisto, Liver tumor-promoting activity of 2,3,7,8-tetrachlorodibenzo-*p*-dioxin (TCDD) in TCDD-sensitive and TCDD-resistant rat strains, Cancer Res. 60 (2000) 6911–6920.

[2] S. Rier, W.G. Foster, Environmental dioxins and endometriosis, Semin. Reprod. Med. 21 (2003) 145–154.

[3] T.S. Thurmond, T.A. Gasiewicz, A single dose of 2,3,7,8-tetrachlorodibenzo-*p*-dioxin produces a time-and dose-dependent alteration in the murine bone marrow B-lymphocyte maturation profile, Toxicol. Sci. 58 (2000) 88–95.

[4] D. Pelclova, Z. Fenclova, Z. Dlaskova, P. Urban, E. Lukas, B. Prochazka, C. Rappe, J. Preiss, A. Kocan, J. Vejlupkova, Biochemical, neuropsychological, and neurological abnormalities following 2,3,7,8-tetrachlorodibenzo-*p*-dioxin (TCDD) exposure, Arch. Environ. Health 56 (2001) 493–500.

[5] U. Simanainen, A. Adamsson, J.T. Tuomisto, H.M. Miettinen, J. Toppari, J. Tuomisto, M. Viluksela, Adult 2,3,7,8-tetrachlorodibenzo-*p*-dioxin (TCDD) exposure and effects on male reproductive organs in three differentially TCDD-susceptible rat lines, Toxicol. Sci. 81 (2004) 401–407.

[6] M.K. Dienhart, R.J. Sommer, R.E. Peterson, A.N. Hirshfield, E.K. Silbergeld, Gestational exposure to 2,3,7,8-tetrachlorodibenzo-*p*-dioxin induces developmental defects in the rat vagina, Toxicol. Sci. 56 (2000) 141–149.

[7] J.G. Hengstler, B. Van der Burg, P. Steinberg, F. Oesch, Interspecies differences in cancer susceptibility and toxicity, Drug Metab. Rev. 31 (1999) 917–970.

[8] D.B. McGregor, C. Partensky, J. Wilbourn, J.M. Rice, An IARC evaluation of polychlorinated dibenzo-p-dioxins and polychlorinated dibenzofurans as risk factors in human carcinogenesis, Environ. Health Perspect. 106 (Suppl. 2) (1998) 755–760.

[9] G.A. Balogh, I.H. Russo, J. Russo, Mutations in mismatch repair genes are involved in the neoplastic transformation of human breast epithelial cells, Int. J. Oncol. 23 (2003) 411–419.

[10] J. Russo, Q. Tahin, M.H. Lareef, Y.F. Hu, I.H. Russo, Neoplastic transformation of human breast epithelial cells by estrogens and chemical carcinogens, Environ. Mol. Mutagen. 39 (2002) 254–263.

[11] Z.Y. Shen, L.Y. Xu, E.M. Li, W.J. Cai, J. Shen, M.H. Chen, S. Cen, S.W. Tsao, Y. Zeng, The multistage process of carcinogenesis in human esophageal epithelial cells induced by human papillomavirus, Oncol. Rep. 11 (2004) 647–654.

[12] T. Kusakari, M. Kariya, M. Mandai, Y. Tsuruta, A.A. Hamid, K. Fukuhara, K. Nanbu, K. Takakura, S. Fujii, C-erbB-2 or mutant Ha-ras induced malignant transformation of immortalized human ovarian surface epithelial cells in vitro, Br. J. Cancer 89 (2003) 2293–2298.

[13] K.S. Kang, I. Morita, A. Cruz, Y.J. Jeon, J.E. Trosko, C.C. Chang, Expression of estrogen receptors in a normal human breast epithelial cell type with luminal and stem cell characteristics and its neoplastically transformed cell lines, Carcinogenesis 18 (1997) 251–257.

[14] J.S. Park, D.Y. Noh, S.H. Kim, G. Kong, C.C. Chang, Y.S. Lee, J.E. Trosko, K.S. Kang, Gene expression analysis in SV40-immortalized human breast luminal epithelial cells with stem cell characteristics using a cDNA microarray, Int. J. Oncol. 24 (2004) 1545–1558.

[15] J.Y. Kim, D. Kim, I. Choi, J.S. Yang, D.S. Lee, J.R. Lee, K. Kang, S. Kim, W.S. Hwang, J.S. Lee, C. Ann, MHC expression in a human adult stem cell line and its down-regulation by hCMV US gene transfection, Int. J. Biochem. Cell Biol. 37 (2005) 69–78.

[16] J.W. Davis 2nd, F.T. Lauer, A.D. Burdick, L.G. Hudson, S.W. Burchiel, Prevention of apoptosis by 2,3,7,8-tetrachlorodibenzo-*p*-dioxin (TCDD) in the MCF-10A cell line: correlation with increased transforming growth factor alpha production, Cancer Res. 61 (2001) 3314–3320.

[17] S. Stinchcombe, A. Buchmann, K.W. Bock, M. Schwarz, Inhibition of apoptosis during 2,3,7,8-tetrachlorodibenzo-*p*-dioxin-mediated tumour promotion in rat liver, Carcinogenesis 16 (1995) 1271–1275.

[18] D. Schrenk, H.J. Schmitz, S. Bohnenberger, B. Wagner, W. Worner, Tumor promoters as inhibitors of apoptosis in rat hepatocytes, Toxicol. Lett. 149 (2004) 43–50.

[19] L.S. Birnbaum, J. Tuomisto, Non-carcinogenic effects of TCDD in animals, Food Addit. Contam. 17 (2000) 275–288.

[20] N.I. Kerkvliet, Recent advances in understanding the mechanisms of TCDD immunotoxicity, Int. Immunopharmacol. 2 (2002) 277–291.

[21] R.C. Gallo, The enigmas of Kaposi's sarcoma, Science 282 (1998) 1837–1839.

[22] N.E. Mueller, A. Mohar, A. Evans, Viruses other than HIV and non-Hodgkin's lymphoma, Cancer Res. 52 (1992) 5479s–5481s.

[23] M.H. Einstein, A.S. Kadish, Anogenital neoplasia in AIDS, Curr. Opin. Oncol. 16 (2004) 455–462.

[24] J.M. Lehmann, G. Riethmuller, J.P. Johnson, MUC18, a marker of tumor progression in human melanoma, shows sequence similarity to the neural cell adhesion molecules of the immunoglobulin superfamily, Proc. Natl. Acad. Sci. U.S.A. 86 (1989) 9891–9895.

[25] C. Bauer, N. Brass, I. Diesinger, K. Kayser, F.A. Grasser, E. Meese, Overexpression of the eukaryotic translation initiation

factor 4G (eIF4G-1) in squamous cell lung carcinoma, Int. J. Cancer 98 (2002) 181–185.

[26] S. Hayashi, K. Nishimura, T. Fukuchi-Shimogori, K. Kashiwagi, K. Igarashi, Increase in cap- and IRES-dependent protein synthesis by overproduction of translation initiation factor eIF4G, Biochem. Biophys. Res. Commun. 277 (2000) 117–123.

[27] K. Tei, N. Kawakami-Kimura, O. Taguchi, K. Kumamoto, S. Higashiyama, N. Taniguchi, K. Toda, R. Kawata, Y. Hisa, R. Kannagi, Roles of cell adhesion molecules in tumor angiogenesis induced by cotransplantation of cancer and endothelial cells to nude rats, Cancer Res. 62 (2002) 6289–6296.

[28] N. Sheibani, W.A. Frazier, Thrombospondin-1, PECAM-1, and regulation of angiogenesis, Histol. Histopathol. 14 (1999) 285–294.

[29] M.J. Humphries, K. Olden, K.M. Yamada, A synthetic peptide from fibronectin inhibits experimental metastasis of murine melanoma cells, Science 233 (1986) 467–470.

[30] Y. Ohtani, H. Kijima, S. Dowaki, H. Kashiwagi, K. Tobita, M. Tsukui, Y. Tanaka, T. Tsuchida, T. Tokunaga, H. Yamazaki, M. Nakamura, Y. Ueyama, M. Tanaka, T. Tajima, H. Makuuchi, Stromal expression of thrombospondin-1 is correlated with growth and metastasis of human gallbladder carcinoma, Int. J. Oncol. 15 (1999) 453–457.

[31] K. Wagner, K. Hemminki, E. Grzybowska, R. Klaes, D. Butkiewicz, J. Pamula, W. Pekala, H. Zientek, D. Mielzynska, E. Siwinska, A. Forsti, The insulin-like growth factor-1 pathway

mediator genes: SHC1 Met300Val shows a protective effect in breast cancer, Carcinogenesis 25 (2004) 2473–2478.

[32] G.M. Clinton, C. Rougeot, J. Derancourt, P. Roger, A. Defrenne, S. Godyna, W.S. Argraves, H. Rochefort, Estrogens increase the expression of fibulin-1, an extracellular matrix protein secreted by human ovarian cancer cells, Proc. Natl. Acad. Sci. U.S.A. 93 (1996) 316–320.

[33] S.B. Gibson, Epidermal growth factor and trail interactions in epithelial-derived cells, Vitam. Horm. 67 (2004) 207–227.

[34] J. DiGiovanni, D.K. Bol, E. Wilker, L. Beltran, S. Carbajal, S. Moats, A. Ramirez, J. Jorcano, K. Kiguchi, Constitutive expression of insulin-like growth factor-1 in epidermal basal cells of transgenic mice leads to spontaneous tumor promotion, Cancer Res. 60 (2000) 1561–1570.

[35] J.V. Thottassery, Y. Sun, L. Westbrook, S.S. Rentz, M. Manuvakhova, Z. Qu, S. Samuel, R. Upshaw, A. Cunningham, F.G. Kern, Prolonged extracellular signal-regulated kinase 1/2 activation during fibroblast growth factor 1- or heregulin beta1-induced antiestrogen-resistant growth of breast cancer cells is resistant to mitogen-activated protein/extracellular regulated kinase kinase inhibitors, Cancer Res. 64 (2004) 4637–4647.

[36] R.I. Fernando, J. Wimalasena, Estradiol abrogates apoptosis in breast cancer cells through inactivation of BAD: Ras-dependent nongenomic pathways requiring signaling through ERK and Akt, Mol. Biol. Cell 15 (2004) 3266–3284.

Gene expression analysis in SV40-immortalized human breast luminal epithelial cells with stem cell characteristics using a cDNA microarray

JOON-SUK PARK[1], DONG-YOUNG NOH[2], SEOK-HYUN KIM[3], SUNG-HOON KIM[4], GU KONG[5],
CHIA-CHENG CHANG[6], YONG-SOON LEE[1], JAMES E. TROSKO[6] and KYUNG-SUN KANG[1]

[1]Laboratory of Stem Cell and Tumor Biology, Department of Veterinary Public Health, College of Veterinary Medicine, Seoul National University, San 56-1, Shilim-Dong, Kwanak-gu, Seoul 151-742; [2]Cancer Research Institute, [3]Department of Obstetrics and Gynecology, College of Medicine, Seoul National University, Seoul 110-799; [4]Graduate School of East-West Medical Science, Kyunghee University, Yongin, Gyeonggi-do 449-701; [5]Department of Pathology, College of Medicine and Molecular Biomarker Research Center, Hanyang University, Seoul 133-791, Korea; [6]Department of Pediatrics and Human Development, Institute of Environmental Toxicology, 246 National Food Safety Toxicology Center, Michigan State University, B-240 Life Sciences Bldg., Michigan State University, East Lansing, MI 48824, USA

Abstract. The epithelial compartment of the human breast comprises two distinct cell types. Type I human breast epithelial cells (HBECs) are expressing luminal epithelial cell markers and stem cell characteristics, whereas Type II HBECs show basal epithelial cell phenotypes. When defined in terms of markers for normal cell lineages, most invasive breast cancer cells correspond to the phenotype of the common luminal epithelial cell. We had developed simian virus 40-immortalized cell lines from normal HBECs with luminal and stem cell characteristics. To identify molecular changes involved in immortalization, we analyzed the differential gene expression profiles of normal and non-tumorigenic immortalized Type I HBECs using cDNA microarray with 7,448 sequence-verified clones. Out of the 7,448 genes screened, consistent gene expression changes among biological replicates included 67 in Type I HBECs and 86 in Type II

HBECs for 4-fold change criteria. Surprisingly, we identified 148 genes (>2.0-fold) as being either up- or down-regulated related to immortalization: 67 genes (*MYBL2, UCHL1 et al*) were up-regulated, and 81 genes (*IGFBP3, CDKN1A et al*) were down-regulated significantly. The altered expression levels of the selected genes were subsequently confirmed by semiquantitative RT-PCR. Our studies suggest that the immortalization of Type I HBECs might be an early step in the initiation of a subset of breast cancer. Furthermore, these results will open up an avenue for more detailed understanding of breast stem cell and tumor biology.

Introduction

Human breast cancer is a complex genetic disease characterized by the accumulation of multiple molecular alterations. The ultimate cure of this disease relies on a better understanding of the mechanisms underlying the initiation and progression of this disease. The neoplastic transformation of HBECs *in vitro* represents a successful model for obtaining knowledge on the molecular and biological alterations that may contribute to the tumorigenic mechanisms. Today, DNA microarray, by allowing the simultaneous and quantitative analysis of the mRNA expression levels of thousands of genes in a single assay, provide novel tools to tackle complexity of this disease. Analysis of pure populations of HBECs at various stages *en route* malignancy would be the direct approach to understanding the cellular and molecular processes of breast carcinogenesis. However, primary cultures of HBECs from breast tissues at various neoplastic stages have been extremely difficult to establish and no cell lines at the intermediate stages of neoplastic transformation are available for mechanistic studies. Normal HBECs do not exhibit spontaneous transformation *in vitro* and thus experimentally-induced transformation of normal HBECs *in vitro* has become

a system of choice to elucidate the mechanism of breast carcinogenesis. Breast carcinomas develop from epithelial cells in the mammary gland. When the phenotype of the invasive cell is defined in terms of markers relating to the normal cell lineages, it is most frequently found to correspond to that of the luminal epithelial cell found in the terminal ductal lobular unit (TDLU) (1,2). For *in vitro* studies on carcinogenesis in the human mammary gland, it is therefore crucial to be able to culture these luminal cells.

We have previously developed a cell culture method to grow two types of normal human breast epithelial cells (HBECs) from reduction mammoplasty (3). The two types of HBECs have been extensively characterized and were found to differ substantially. The HBECs with stem cell characteristics (Type I HBECs) described in this study were discovered by a distinguishable cell and colony morphology associated with these cells which are different from the conventional cell type (Type II HBECs) (4; Chang *et al*, Proc Am Assoc Cancer Res 37: abs. 38, 1996). After characterization, Type II HBECs, similar to those commercially available or used by most other laboratories, shows basal epithelial cell markers (3,5). Type I HBECs were found to possess major stem cell features (i.e., ability to differentiate into Type II HBECs by cyclic AMP-inducing agents (cholera toxin and forskolin) and to form budding/ductal structure in Matrigel) (3,7). Because mammary stem cells are known to be present in the end bud for ductal morphogenesis and elongation (8,9), the ability of Type I HBECs to form these structures strongly indicates that the Type I HBEC population partially contains mammary epithelial stem cells which are capable of giving rise to luminal and basal epithelial cells (10,11). In addition, Type I HBECs are characterized by their lack of connexin 26 and 43 expression, functional gap junction intercellular communication (GJIC) and the expression of epithelial membrane antigen (EMA), keratin 18 and 19, and the non-expression of keratin 14 and integrin alpha 6 (ITGA6) (3,7,10,11). Connexin 43 can serve as a negative marker for epidermal stem cells (10). GJIC deficiency has been reported to be a characteristic of putative stem cells (3,10,12-15). Multipotent progenitor cells of the human breast reside in a predominantly keratin K19+ compartment (16).

According to the stem cell theory of carcinogenesis, stem cells give rise to cancer cells by blocking their differentiation and preserve the undifferentiated characteristics of stem cells in cancer cells (8,15,17). These results support the concept of cancer as oncogeny as blocked or partially blocked ontogeny (18). Recently, the field of stem cell biology has attracted increasing attention because of the suggestion that adult stem cells might have a broader potential or plasticity than was previously considered (19,20).

The induction of immortalization of normal HBECs has been reported previously (3-6). Importantly, two types of HBECs differ substantially in their response to an oncogenic (SV40) stimuli, i.e. Type I HBECs have a greater tendency to become immortal and, most strikingly, have the ability to grow in soft agar (AIG+); SV40-transfected Type II HBECs totally lack the ability to grow in soft agar (AIG-). In addition, our SV40-immortalized Type I HBECs were shown to be non-tumorigenic when inoculated into athymic nude mice.

Inactivation of the p16/pRb and p53 pathway is necessary to bypass senescence; because the function of SV40 large T-antigen is to inactivate p53 and pRb and to induce the CCAAT box binding factor that transactivates cell cycle-regulating genes such as cdc2 (21), alteration in cell cycle regulation seems to be the major event to acquire an extend lifespan (EL) for normal HBECs. However, this is insufficient for immortalization. The subsequent conversion of a cell with EL to an immortal cell clearly involves the activation of telomerase, although the overexpression of telomerase alone is not sufficient to confer immortalization in epithelial cells (4,22). In addition, genetic analyses of immortalized HBECs reveal that a number of consistent genetic alteration are required.

To gain insight into candidate genes or novel pathways involved in immortalization, we have investigated the gene expression alterations that take place during the SV40-immortalization of Type I HBECs with stem cell properties using cDNA microarray with 7,448 sequence-verified clones. Because SV40-immortaliztion was more effective in Type I HBECs than Type II HBECs and Type I HBECs described in the past studies might be the major target cell for neoplastic transformation (3,4), our study focused on SV40-immortalization of Type I HBECs. We have identified several genes related to immortalization, *MYBL2* and *UCHL1*, that are up-regulated, and *CDKN1A* and *IGFBP3*, that are inactivated. These data support the concept that molecular pathways selectively involved in immortalization are important in carcinogenesis and tumor progression.

Materials and methods

Cells and cell culture. Normal HBECs were isolated from primary cultures of biopsies from patients undergoing reduction mammoplasty for cosmetic reasons, and from residual tissue from mastectomy specimens with breast carcinoma. The media and the procedure used to develop the two types of normal HBECs have been described previously (3). Briefly, it was mechanically disaggregated followed by enzymatic disaggregation with collagenase to release epithelial organoid. The primary cultures developed *in vitro* for one week were stored in liquid nitrogen. During this 1 week period, virtually all of the fibroblasts can be removed by treatment (1-2 times) with diluted trypsin-EDTA solution. Early passage cells, after recovery from liquid nitrogen storage, were used in these experiments. All cell cultures were grown at 37°C in incubators supplied with 5% CO_2 and humidified air. The first passage cells, subcultured from the initial culture, were thawed from the preserved cells in liquid nitrogen, when cultured in FBS-free MSU-1 medium, formed two morphologically distinguishable colonies. The first passage of HBECs recovered from liquid nitrogen storage, was plated in MSU-1 medium supplemented with 5% FBS for 3 h for the attachment of residual fibroblast. The epithelial cells in suspension were transferred to new plates and cultured in FBS-free MSU-1 medium. After overnight culture, the cells that remained in suspension were transferred to new plates. Continued culture of these last transferred cells in FBS-containing MSU-1 medium gave rise to one morphological type of cell. The attached cells, in the overnight culture,

cultured in FBS-free MSU-1 medium supplemented with 0.4% bovine pituitary extract gave rise to a second morphological type of cell. The rare contaminants of the other cell type in these cultures were removed by mechanically scraping the unwanted small colonies once they were morphologically recognizable.

Transformation of normal Type I HBEC was achieved by lipofectin-mediated transfection of HBEC with SV40 DNA (Gibco-BRL) (M13SV1 derived from normal HBEC cultures HME-13). The SV40-transformed immortal Type I HBEC-derived cell line (M13SV1) reported previously was non-tumorigenic (3,5-7,23). Developing colonies after SV40 transfection were isolated by the trypsin/glass ring method for further characterization. SV40-transfected HBECs which were propagated continuously (a cumulative population doubling level >100) are referred to as being immortal.

The normal HBECs with the two different types of morphology and M13SV1 can be monitored microscopically daily and easily distinguished under a phase contrast microscope (Olympus CK-2, Okaya, Japan). Transmitted (phase contrast) images were acquired using IX-70 microscope (Olympus, Okaya, Japan) with a digital camera (JENOPTIK ProgRes C14, Munich-Eching, Germany). Cells were analyzed microscopically at x200 and x400 magnification.

cDNA microarray preparation. The cDNA microarrays used in this study were constructed at the GenomicTree, Inc. (Daejon, Korea) (24). A set of 7,448 sequence-verified human cDNA clones was purchased from Research Genetics, Inc. (Huntsville, AL, USA). Bacterial clones were amplified in 96-well culture plates. Plasmid DNA was isolated using a Millipore plasmid kit (Millipore, Bedford, MA, USA) and ORFs were PCR-amplified using a pair of universal primers, 5'-CTGCAAGGCGATTAAGTTGGGTAAC-3' and 5'-GTGAGCGGATAACAATTTCACACAGGAAACAGC-3' under the following conditions: initial denaturation at 94°C for 2 min, followed by 30 cycles of 94°C for 45 sec, 55°C for 45 sec and 72°C for 2 min, and a final extension step at 72°C for 10 min. The PCR amplification products were examined by 1% agarose gel electrophoresis, purified using a Sephadex G-50 column, dried and then resuspended in a 50% DMSO solution. DNA was spotted by an OmniGrid™ Microarrayer (GeneMachines, Inc., San Carlos, CA, USA) onto a silanized glass slide surface (CMT-GAPS™, Corning, Charlotte, NC, USA). Some of the genes, including the GAPDH control, were spotted more than once in the microarray so that 7,448 unique genes, including ESTs, were represented by 7,775 spots in each microarray. Each slide was crosslinked with 300 mJ short wave UV irradiation (Stratalinker, Stratagene, La Jolla, CA, USA) and stored in a desiccator until use.

Total RNA isolation, target preparation and hybridizations. The two cellular types of HBECs and M13SV1 were plated on 100 mm plastic dishes. Culture medium was changed once every 2 days. Total cellular RNA was extracted from cells grown to about 50-70% confluence or 5-10 mm HBECs population's diameter by using TRIzol Reagent™ (Invitrogen, Carlsbad, CA) according to the manufacturer's instructions. The extracted RNA was dissolved in RNase-free water, and its concentration and purity were determined from absorbance

measurements at 260 and 280 nm using a spectrophotometer. Quality of the RNA was checked by visualizaion of the 28S:18S ribosomal RNA ratio on a 1% agarose gel. The overall procedure of hybridization was performed according to manufacturer's instructions (GenomicTree, Inc.) as described in previous study (24). Briefly, 100 μg each of total RNA from Type I HBECs, Type II HBEC, M13SV1 was reverse-transcribed using oligo-dT primers (5'-TTTTTTTTTTTTTTTT TTTTTVN-3') in the presence cyanine 3-dUTP or cyanine 5-dUTP (NEN Life Science Products, Boston, MA), respectively by using Superscript II Reverse Transcriptase (Life Technologies. Inc.). The labeled cDNA probe was then purified through a microcon-30 column and resuspended in 80 μl of hybridization solution (3X SSC and 0.3% SDS). The probe was then denatured at 100°C for 2 min and applied to the DNA chip at 65°C for 16 h in a humidified chamber. Finally the hybridized slide was washed once each in 2X SSC for 2 min, 0.1X SSC/0.1% SDS for 5 min, and 0.1X SSC for 5 min and then spun-dried prior to scanning at room temperature.

Data acquisition and analysis. Fluorescent cDNA probes hybridized to a cDNA microarray were detected by scanning the slide with a GenePix 4000A scanner (Axon instruments, Inc., Foster City, CA). The Cy5- and the Cy3-labeled cDNA samples were scanned at 635 and 532 nm, respectively, to obtain images of 10-μm resolution. The resulting TIFF images were analyzed and the quantification of spot intensities, qualities, and local background was performed automatically by the GenePix Pro 3.0 software package (Axon Instruments, Inc., Foster City, CA) using variable spot diameter in the range 70-180 μm and a manual supervision for any inaccuracies in the automatic spot detection. Scanning was repeated until the center of ratio distributes to 1 by increasing or decreasing the photomutiplier tubes (PMT) voltage. The expression intensity information for all genes was exported into Microsoft Excel spreadsheet. The raw fluorescent signal intensity values were initially subjected to a spot quality filter to ensure the accuracy of the expression ratios. Data were globally normalized to make the median value of the log2-ratio equal at zero. Expression values were normalized by a single multiplicative normalization factor for each ratio result (ratio of medians, ratio of means, median of ratios, mean of ratios, and regression ratio) and applied to all Cy5/Cy3 ratios so that the median normalized Cy5/Cy3 ratio became 1.0 (25). Poor quality spots (sum of median <1000) were filtered from the raw data before analysis. For each hybridized spot, gene expression value (GEV; ratio of median in GenePix pro 3.0), a ratio of Cy5 fluorescence intensity minus Cy5 background intensity to Cy3 fluoresence intensity minus Cy5 background intensity, is calculated and represents a fold gene expression change for each gene. The cDNA microarray experiments were repeated at least twice at each condition and the average of two GEVs for each gene was used for the analysis.

Reverse transcription-polymerase chain reaction (RT-PCR) analysis. The first-strand cDNA was generated from 2 μg of total RNA by RT with 1 μl poly dT primer (12-18 mer) and 50 U SuperScript II RNase H⁻ Reverse Transcriptase in a 20 μl reaction mixture as described (Life Technologies, Inc.).

Table I. Primer pairs used for RT-PCR.

Gene name	Primer sequence (5'~3')	PCR product size (bp)
Up-regulated in Type II HBECs		
ITGA6	Forward: GGAGCAACAGCAAACAGGTG	388
	Reward: GTTGACCACCCTCCCAACAC	
K14	Forward: AGCTGTATTGATTGCCAGGAG	252
	Reward: CGCAGTCATCCAGAGATGTG	
Up-regulated in Type I HBECs		
TAGLN	Forward: CACACCCGTGTGGTACCTTC	282
	Reward: GCTGGGCTGGTTCTTCTTC	
RAI3	Forward: CTGTCCCCAAACTTGCTGTC	311
	Reward: GCCACCACCATGAAAGAGTG	
IGFBP3	Forward: GAGCCCATCCAGGACACTG	337
	Reward: GTGTFTCCACACCGAGGTC	
EMP1	Forward: AAGGAAATGTTGAGGGCAAG	292
	Reward: GAACAATCCACCAGAGTAATGC	
K8	Forward: GGCTATGCAGGTGGTCTGAG	356
	Reward: GGGGTCCCCAGGTAGTAAAC	
Up-regulated genes in M13SV1		
SLC26A2	Forward: GGTTTCAGGCTTTCTTGCAG	318
	Reward: GGAGCAAAGACTGGGGATAG	
UCHL1	Forward: GGATGGCCACCTCTATGAAC	296
	Reward: GCGTGTCTGCAGAACAGAAG	
MYBL2	Forward: CCTGAGGTGTTGAGGGTGTC	324
	Reward: CCCATCCTAAGCAGGGTCTG	
Housekeeping gene		
GAPDH	Forward: CTGCACCACCAACTGCTTAG	222
	Reward: TTCAGCTCAGGGATGACCTT	

Abbreviations: ITGA6, integrin alpha 6; K14, keratin 14; TAGLN, transgelin; RAI3, retinoic acid induced 3; IGFBP3, insulin-like growth factor binding protein 3; EMP1, epithelial membrane protein 1; K8, keratin 8; SLC26A2, solute carrier family 26 (sulfate transporter), member 2; UCHL1, ubiquitin carboxyl-terminal esterase L1; MYBL2, v-myb avian myeloblastosis viral oncogene; MME, membrane metallo-endopeptidase; GAPDH, glyceraldehyde 3-phosphate dehydrogenase.

PCR was carried out in a 50 μl reaction containing 25 mM MgCl$_2$, 10 mM dNTP mix, 10 μM of each primer set, 2.5 U of *Taq* polymerase, and 2 μl of cDNA template (from a total of 20 μl produced). PCR amplification was performed using a Hybaid DNA thermal cycler. After hot start at 94°C for 2 min, PCR was programmed as follows: denaturing at 94°C for 45 sec, annealing at 57-65°C for 45 sec, and extension at 72°C for 30 sec. The PCR reaction conditions and cycle numbers were individually optimized and adjusted so that the reactions fell within the linear range of product amplification (9). After the final cycle, we used a 5-min extension period at 72°C. The glyceraldehyde 3-phosphate dehydrogenase (GAPDH) was used in each RNA sample to amplify GAPDH cDNA as a reference under the same PCR conditions. PCR products were analyzed by electrophoresis through 2% agarose gels containing 0.1 mg/ml of ethidium bromide. Images of the RT-PCR ethidium bromide-stained agarose gels were acquired with UV illumination on a GelDoc2000/ChemiDoc System (Bio-Rad) and quatification of the bands was performed by densitometry using the Quantity One software (version 4.0.1; Bio-Rad). Primer sequences are found in Table I.
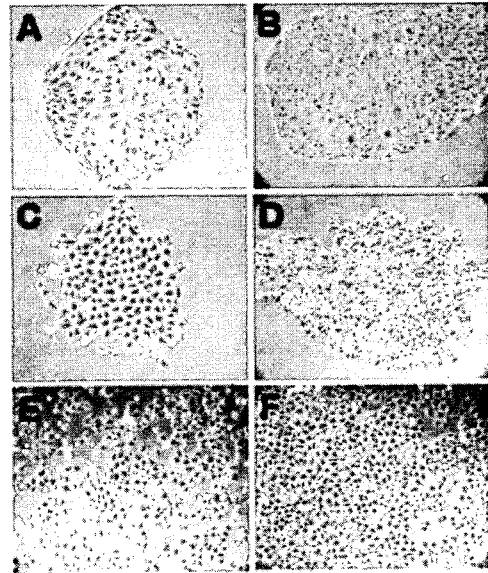
Figure 1. Two types of HBEC colonies and M13SV1 grown in MSU-1 medium. Type I HBECs' colonies were developed in 5% FBS-containing MSU-1 medium for 5 days (A) and 7 days (B). Type II HBEC colonies were cultured in FBS-free MSU-1 medium supplemented with 0.4% BPE for 5 days (C) and 7 days (D). M13SV1 seeded at 1x10^5 cells/cm^2 reach 60-70% and 90-100% confluency at 1 and 2 days, respectively (E and F). The edge of Type I HBEC colonies was smooth and appears to be bounded by a layer of elongated cells, in contrast to the rough and non-constrained outline of Type II HBEC colonies. The shape of Type I HBECs was a more variable and spread, while it of Type II HBECs was uniform and compact. Original magnification: (A) and (C), x400; (B), (D), (E) and (F), x200.

Results

Characterization of HBECs. The two types of HBECs have been extensively characterized and were found to differ substantially in phenotypes (Figs. 1 and 2). Normal HBECs were isolated from different reduction mammoplasty tissue specimens. The Type I and Type II HBECs derived from these specimens are morphologically distinguishable (Fig. 1). Type I HBECs contained cells that were elongated and variable in shape and less reflective and less distinctive in cell boundary (Fig. 1A and B). Type II HBECs contained cells that were more uniform in cell shape (cobble stone-shaped) and have a conspicuous cell boundary (Fig. 1C and D). Type I HBEC colonies are smooth and appear to be bounded by a layer of elongated cells, in contrast to the non-constrained outline of Type II HBEC colonies (3).

Differential gene expression analysis by cDNA microarray. We have analyzed the relative expression levels of 7,448 genes and EST represented on our arrays in an attempt to identify genes related to immortalization of Type I HBEC, as described in Materials and methods. Sum of medians indicates the sum of the median intensities for each wavelength, with the median background at each wavelength subtracted. In other words, it means signal intensity of both

A   B

	Type II	Type I	M13SV1
ITGA6	15.93	1.00	LS
K14	2.49	1.00	-2.90
TAGLN	-10.92	1.00	-12.74
RAI3	-31.20	1.00	-2.74
IGFBP3	-33.03	1.00	-13.16
EMP1	-5.08	1.00	-4.61
K8	-2.88	1.00	1.35
SLC26A2	-1.08	1.00	5.69
UCHL1	-1.01	1.00	35.65
MYBL2	-5.56	1.00	8.09
GAPDH			

Figure 2. Confirmation by RT-PCR of microarray results using RNA from Type I, II HBECs and M13SV1. (A), *TGA6* (35), *K14* (30), *TAGLN* (32), *RAI3* (34), *IGFBP3* (33), *EMP1* (32), *K8* (34), *SLC26A2* (32), *UCHL1* (30), *MYBL2* (30), *GAPDH* (32) were amplified and products were separated in a 2% agarose gel and stained with ethidium bromide. The number in parentheses indicates PCR cycles. RT-PCR was carried out under linear amplification conditions. *GAPDH* was used as the control for equivalent, RNA template among the three samples in the PCR reactions. (B), The fold change of microarray analysis was calculated from the mean of biological triplicates. LS (low signal): signal intensities ≤500.
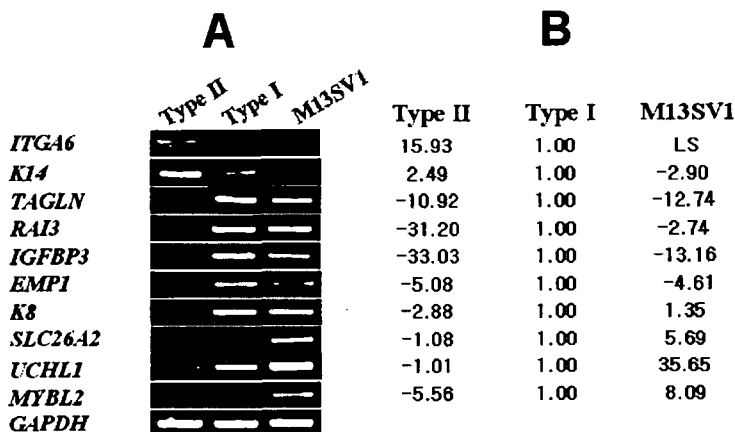
channels. In order to obtain reliable and detectable expression of the represented genes and ESTs, genes with sum of medians <1000 were eliminated. Each hybridization to compare gene expression changes in Type I versus Type II HBECs, Type I HBECs versus M13SV1 (SV40-transformed immortal Type I HBEC-derived cell line) resulted in ~40% of probe sets showing detectable gene expression. The percentage of differentially expressed genes was 2.05% (153 out of a total of 7,448 genes) between Type I and Type II HBECs and 1.99% (148/7,448 genes) between Type I HBECs and M13SV1. Among the total of 153 differentially expressed genes, 67 of the changes were specific for Type I, and 86 were specific for Type II HBECs (Table II). Sixty-seven out of 148 genes were up-regulated in non-tumorigenic immortalized M13SV1 (Table III), while 81 were down-regulated (Table IV). Genes were assigned to functional categories using SOURCE provided by the Genetics Department, Stanford University (http://genome-www5. stanford.edu/cgi-bin/SMD/ sourceSearch/). Data on this page are curated from UniGene, Swiss-Prot, GeneMap99, RHdb and LocusLink. The pattern of expression and identity of these genes is shown in Tables II, III and IV.

Validation of cDNA microarray results. Although our chip provided a screen for differentially expressed genes based on consistent performance in the biological duplicates, false-positive results due to limitations of the technologies (26) might obscure the true biological variations. Therefore, semi-quantitative RT-PCR analysis was performed for the 11 randomly chosen genes in order to verify the identity of these genes shown in Tables II, III and IV and to set the reliability of the microarray data. Although *K14* and *K8* were excluded in Table II, proteins encoded by these genes are known for markers which express characteristic phenotype in HBECs. Therefore, these might be also overexpressed in mRNA

levels. Although *SLC26A2* were also excluded in Table II, RT-PCR was executed to verify the data of microarray. The trend of the amplification intensity measured by the RT-PCR approach correlated with the findings by microarray analysis in that *ITGA6* and *K14* were overexpressed in Type II HBEC, while *TAGLN*, *RAI3*, *IGFBP3*, *EMP1*, and *K8* in Type I HBEC, and *SLC26A2*, *UCHL1*, and *MYBL2* in M13SV1 (Fig. 2). These results indicate that a qualitative correlation existed between RT-PCR and the microarray data.

Chromosomal locations in normal and immortal HBECs. All of 67 genes enriched in Type I HBECs have been mapped to a chromosomal location in LocusLink (NCBI), while 82 of 86 genes enriched in Type II HBECs have been done. Of 148 genes expressed in M13SV1, 142 have been done (65 up- and 77 down-regulated genes). Since mapping information was obtained, values on the y-axis were normalized for each chromosome to the total number of genes/chromosome mapped in LocusLink (Fig. 3).

Type II HBEC-enriched genes were mainly located in chromosomes 18, 9 and 7, but Type I HBEC-enriched genes were mainly located in chromosomes 21, 20, 12, 11 and 6 (Fig. 3A). The most common genomic change in SV40-immortalized human cells is the loss of chromosome 6 (27). Recently, alterations at several other chromosomal loci (e.g. 20q13.2, 6q26-27) have been implicated in immortalization of various epithelial cells with viral oncogenes (28,29). Genes up-regulated in M13SV1 were situated in chromosomes 14, 20, 2 and 17 (Fig. 3B), while genes down-regulated in M13SV1 were situated in chromosomes 1, 12, 11 and 6.

Discussion

In this study, we have analyzed the gene expression profiles of two types of HBECs and SV40-immortalized cell lines

Table II. Functional classification of differentially expressed genes between Type I and Type II HBECs.[a]

Functional class	Accession no.[b]	Gene description	Function[c]	Chromosome location	GEV[d] T I	T II
Extracellular matrix						
CDH2	W49619	Cadherin 2, type 1, N-cadherin (neuronal)	Cell adhesion	18q11.2	20,437	
CLDN4	AA430665	Claudin 4	Tight junction	7q11.23	15,712	
COL1A2	AA490172	Collagen, type I, alpha 2	ECM protein	7q22.1	10,317	
OSF-2	AA598653	Osteoblast specific factor 2 (fasciclin I-like)	Cell adhesion	13q13.2	7,971	
MMP7	AA031514	Matrix metalloproteinase 7 (matrilysin, uterine)	ECM remodeling	11q21-q22	7,931	
CLDN7	AA487488	Claudin 7	Tight junction	17p13	4,895	
LAMR1	AA629897	Laminin receptor 1 (ribosomal protein SA, 67 kDa)	Laminin receptor	3p21.3	4,398	
DSG3	AI582245	Desmoglein 3 (pemphigus vulgaris antigen)	Cell adhesion	18q12.1-q12.2		19,466
CDH13	R41787	Cadherin 13, H-cadherin (heart)	Cell adhesion	16q24.2-q24.3		19,170
ITGA6[e]	R43483	Integrin, alpha 6	Cell-cell matrix adhesion	2q31.1		15,930
DSG1	AA041388	Desmoglein 1	Cell adhesion	18q12.1		13,253
TGM1	AI652954	Transglutaminase 1	Membrane fraction	14q11.2		8,292
COL7A1	AA598507	Collagen, type VII, alpha 1 (epidermolysis bullosa)	ECM protein	3p21.1		5,634
LAMA3	AA001432	Laminin, alpha 3	Basement membrane components	18q11.2		5,487
DSP	H90899	Desmoplakin (DPI, DPII)	Cell-cell adherens junction	6p24		4,044
Cell shape and motility						
CTGF	AA598794	Connective tissue growth factor	Cell motility	6q23.1	12,051	
MYL9	AA877166	Myosin, light polypeptide 9, regulatory	Structural protein of muscle	20q11.22	6,751	
K-ALPHA-1	AA865469	Tubulin, alpha, ubiquitous	Structural protein	12q12-12q14.3	4,949	
TUBB	AW081868	Tubulin, beta polypeptide	Cytoskeletal structural protein	6p21.3	4,430	
BPAG1	H44785	Bullous pemphigoid antigen 1, 230/240 kDa	Cytoskeleton organization	6p12-p11		35,586
Cell cycle						
CCND1	AA487486	Cyclin D1 (PRAD1: parathyroid adenomatosis 1)	G1-S regulation	11q13	5,732	
Development and differentiation						
ENC1	AA100036	Ectodermal-neural cortex (with BTB-like domain)	Neurogenesis	5q12-q13.3	12,260	
TAGLN[e]	AI668906	Transgelin	Muscle development	11q23.2	10,924	
HOXA4	AA449704	Homeo box A4	Embryogenesis	7p15-p14	7,930	
KLK7	AI139437	Kallikrein 7 (chymotryptic, stratum corneum)	Epidermal differentiation	19q13.41	6,809	
EMP1[e]	AA975768	Epithelial membrane protein 1	Epidermal differentiation	12p12.3	5,084	
SPRR1A	AI923984	Small proline-rich protein 1A	Epidermal differentiation	1q21-q22		64,208
FEZ1	H20759	Fasciculation and elongation protein zeta 1 (zygin I)	Neurogenesis	11q24.2		14,184
MYO1B	AA047778	Myosin IB	Neuronal development	2q12-q34		5,500
CYP1B1	AA448157	Cytochrome P450, subfamily I, polypeptide 1	Eye morphogenesis	2p21		5,298
DKK3	AA425947	Dickkopf homolog 3 (Xenopus laevis)	Embryogenesis and morphogenesis	11p15.2		4,157
Cell growth						
RARRES1	N94424	Retinoic acid receptor responder (tazarotene induced) 1	Negative control of cell proliferation	3q25.31	27,439	
CYR61	AA777187	Cysteine-rich, angiogenic inducer, 61	Cell proliferation	1p31-p22	10,165	
RARRES3	W47350	Retinoic acid receptor responder (tazarotene induced) 3	Negative control of cell proliferation	11q23	7,942	
QSCN6	AA464152	Quiescin Q6	Cell cycle control	1q24	4,972	
BAP1	H09066	BRCA1 associated protein-1	Negative control of cell proliferation	3p21.31-p21.2	4,971	
GPNMB	AA425450	Glycoprotein (transmembrane) nmb	Negative control of cell proliferation	7p15		25,691
AREG	AA857163	Amphiregulin (schwannoma-derived growth factor)	Cell proliferation	4q13-q21		5,546
Immune						
IFIT2	N63988	Interferon-induced protein with tetratricopeptide repeats 2	IFN-induced protein	10q23-q25	13,436	
NK4	AA458965	Natural killer cell transcript 4	Immune response	16p13.3	11,647	
G1P3	AA448478	Interferon, alpha-inducible protein (clone IFI-6-16)	IFN-induced protein	1p35	11,598	
IFIT1	AA489640	Interferon-induced protein with tetratricopeptide repeats 1	IFN-induced protein	10q25-q26	10,655	
CD24	H59916	CD24 antigen (small cell lung carcinoma cluster 4 antigen)	Humoral defense mechnisme	6q21	8,931	
ISG15	AA406020	Interferon-stimulated protein, 15 kDa	IFN-induced protein	1p36.33	5,473	
HLA-C	AA464246	Major histocompatibility complex, class I, C	Immune response	6p21.3	4,485	
C1S	T62048	Complement component 1, s subcomponent	Immune response	12p13		15,727
C1R	T69603	Complement component 1, r subcomponent	Immune response	12p13		8,706
HLA-DQB1	AA458472	Major histocompatibility complex, class II, DQ beta 1	Immune response	6p21.3		8,532
APOH	W06980	Apolipoprotein H (beta-2-glycoprotein I)	Defense/immunity protein	17q23-qter		8,483
HLA-DQB1	AA669055	Major histocompatibility complex, class II, DQ beta 1	Immune response	6p21.3		5,309
Metabolism						
GSTA2	T73468	Glutathione S-transferase A2	Detoxication enzyme	6p12.1	25,355	
ALDH1A3	AA455235	Aldehyde dehydrogenase 1 family, member A3	Lipid metabolism	15q26.3	8,476	
ENO2	AA450123	Enolase 2, (gamma, neuronal)	Glycolysis	12p13	4,684	
ALDH1B1	R93551	Aldehyde dehydrogenase 1 family, member B1	Carbohydrate metabolism	9p13	4,268	
AKR1C1	AI924357	Aldo-keto reductase family 1, member C1	Xenobiotic metabolism	10p15-p14		13,620
AKR1C1	R93124	Aldo-keto reductase family 1, member C1	Xenobiotic metabolism	10p15-p14		13,236
AKR1C3	AA916325	Aldo-keto reductase family 1, member C3	Lipid metabolism	10p15-p14		9,311
ALOX15B	AI858088	Arachidonate 15-lipoxygenase, second type	Fatty acid metabolism	17p13.1		9,012
ABCA1	AA521292	ATP-binding cassette, sub-family A (ABC1), member 1	Cholesterol metabolism	9q31.1		8,814
MAOA	AA011096	Monoamine oxidase A	Biogenic amine metabolism	Xp11.4-p11.3		6,736
PRNP	AA455969	Prion protein (p27-30) (Creutzfeld-Jakob disease)	Metabolism	20pter-p12		4,496
AKR1B10	AI924753	Aldo-keto reductase family 1, member B10	Steroid metabolism	7q31.31		4,323
Protein degradation						
TIMP3	AA099153	Tissue inhibitor of metalloproteinase 3	Proteolysis and peptidolysis	22q12.3		9,418
PRSS3	AI308916	Protease, serine, 3 (mesotrypsin)	Proteolysis and peptidolysis	9p11.2		7,552
PRSS2	AA284528	Protease, serine, 2 (trypsin 2)	Proteolysis and peptidolysis	7q34		4,999
Transcription						
ID4	AA464856	Inhibitor of DNA binding 4	Transcription co-repressor	6p22-p21	6,043	
MYBL2[e]	AA457034	V-myb myeloblastosis viral oncogene homolog-like 2	Transcription factor	20q13.1	5,559	
JUND	AA131585	Jun D proto-oncogene	Transcription regulation	19p13.2		10,763
SNAI2	N64741	Snail 2	Transcription activating factor	8q11		7,901
HLXB9	AI738662	Homeo box HB9	RNA polymerase II transcription factor	7q36		7,565
PIR	H69335	Pirin	Transcription co-factor	Xp21.3		5,340
NFIL3	AA633811	Nuclear factor, interleukin 3 regulated	Transcription factor	9q22		4,952
MAF	AA043501	V-maf musculoaponeurotic fibrosarcoma oncogene homolog	RNA polymerase II transcription factor	16q22-q23		4,856
DSIPI	AA775091	Delta sleep inducing peptide, immunoreactor	Transcription factor	Xq22.3		4,752
Signaling						
IGFBP3[e]	AA598601	Insulin-like growth factor binding protein 3	Signal transduction	7p13-p12	33,028	
RAI3[e]	AA172400	Retinoic acid induced 3	Signal transduction	12p13-p12.3	31,199	
GUCY1A3	H24329	Guanylate cyclase 1, soluble, alpha 3	Signal transduction	4q31.1-q31.2	27,097	
LIF	R50354	Leukemia inhibitory factor	Cell-cell signaling	22q12.2	12,030	

Table II. Continued.

Functional class	Accession no.[b]	Gene description	Function[c]	Chromosome location	GEV[d] T I	T II
CXCL6	AI889554	Chemokine (C-X-C motif) ligand 6	Signal transduction	4q21	9,441	
MX1	AA457042	Myxovirus (influenza virus) resistance 1	Signal transduction	21q22.3	8,682	
DKK1	AA253464	Dickkopf homolog 1 (Xenopus laevis)	Signal transduction	10q11.2	5,132	
DDAH1	AA456324	Dimethylarginine dimethylaminohydrolase 1	NO mediated signal transtuction	1p22	4,977	
AKT1	AA464217	V-akt murine thymoma viral oncogene homolog 1	Signal transduction	14q32.32	4,515	
FZD7	N69049	Frizzled homolog 7 (Drosophila)	Frizzled receptor signalling pathway	2q33	4,017	
EPIM	AA056536	Epimorphin	Signal transduction	7		19,319
HBP17	AA936757	Heparin-binding growth factor binding protein	Cell-cell signaling	4p16-p15		18,585
VAV3	H10045	Vav 3 oncogene	Signal transduction	1p13.2		16,248
PTPN13	AA679180	Protein tyrosine phosphatase, non-receptor type 13	Protein dephosphorylation	4q21.3		15,025
FLRT3	AA456022	Fibronectin leucine rich transmembrane protein 3	Signal transduction	20p11		13,568
MTA1	N71159	Metastasis associated 1	Signal transduction	14q32.3		12,058
EGFR	W48713	Epidermal growth factor receptor	EGF receptor signalling pathway	7p12		11,595
IMPA2	R42685	Inositol(myo)-1(or 4)-monophosphatase 2	Signal transduction	18p11.2		9,157
GJB2	AA490466	Gap junction protein, beta 2, 26 kDa (connexin 26)	Cell-cell signalling	13q11-q12		8,104
GAB1	N68193	GRB2-associated binding protein 1	EGF receptor signalling pathway	4q28.3		8,027
GNG10	R62817	Guanine nucleotide binding protein 10	Signal transduction	9q32		5,406
MME	R98936	Membrane metallo-endopeptidase (CALLA, CD10)	cell-cell signaling	3q25.1-q25.2		4,599
ADM	AA446120	Adrenomedullin	Signal transduction	11p15.4		4,554
IGFBP6	AA478724	Insulin-like growth factor binding protein 6	Signal transduction	12q13		4,535
PTK2	AA630298	PTK2 protein tyrosine kinase 2	Integrin receptor signalling pathway	8q24-qter		4,422
Stress						
GSTA3	N30096	Glutathione S-transferase A3	Stress response	6p12.1	10,248	
GSTT1	H99813	Glutathione S-transferase theta 1	Stress response	22q11.23	6,712	
GSTA4	AA152347	Glutathione S-transferase A4	Stress response	6p12.1		8,560
SOD2	AA488084	Superoxide dismutase 2, mitochondrial	Oxidative stress response	6q25.3		7,468
S100A2	AA458884	S100 calcium binding protein A2	Stress response	1q21		5,162
Transport						
LCN2	AA400973	Lipocalin 2 (oncogene 24p3)	Transport of small lipophilic substances	9q34	8,519	
SCNN1B	AI346878	Sodium channel, nonvoltage-gated 1, beta	Sodium transport	16p12.2-p12.1	6,579	
FOLR1	R24530	Folate receptor 1 (adult)	Folate transport	11q13.3-q14.1	6,201	
TMEM1	N65981	Transmembrane protein 1	Sodium transport	21q22.3	5,504	
SLC5A6	AA186605	Solute carrier family 5, member 6	Multivitamin transporter	2p23	4,078	
GPX2	AA135152	Glutathione peroxidase 2 (gastrointestinal)	Electron transporter	14q24.1		5,547
ARF4L	H15085	ADP-ribosylation factor 4-like	Non-selective vesicle transport	17q12-q21		5,406
SLC38A2	AA598996	Solute carrier family 38, member 2	Amino acid transport	12q		5,354
SLC1A5	AI973241	Solute carrier family 1, member 5	Neutral amino acid transport	19q13.3		4,839
SLC16A1	AA043133	Solute carrier family 16, member 1	Mevalonate transport	1p12		4,464
Miscellaneous						
ANPEP	T73440	Alanyl (membrane) aminopeptidase (CD13, p150)	Receptor	15q25-q26	16,534	
MFI2	AA974052	Antigen p97 (melanoma associated)	Tumor antigen	3q28-q29	10,594	
PRG1	AA278759	Proteoglycan 1, secretory granule	Proteoglycan	10q22.1	9,874	
NPR1	AA598841	Natriuretic peptide receptor A/guanylate cyclase A	Receptor	1q21-q22	5,021	
PLAT	AA447797	Plasminogen activator, tissue	Blood coagulation	8p12	4,994	
KLK10	AA459401	Kallikrein 10	Serine-type peptidase	19q13.3-q13.4	4,442	
TP63	AA455929	Tumor protein p63	Induction of apoptosis	3q27-q29		25,490
CA12	AA171613	Carbonic anhydrase XII	Carbonate dehydratase	15q22		16,996
SERPINB3	AA398883	Serine proteinase inhibitor, clade B (ovalbumin), member 3	Serine protease inhibitor	18q21.3		12,647
CSTA	W72207	Cystatin A (stefin A)	Proteinase inhibitor	3q21		10,163
SERPINB5	AI989728	Serine proteinase inhibitor, clade B (ovalbumin), member 5 (maspin)	Serine protease inhibitor	18q21.3		9,504
PDCD4	N71003	Programmed cell death 4	Apoptosis	10q24		6,373
PLA2R1	AA086038	Phospholipase A2 receptor 1, 180 kDa	Inflammatory response	2q23-q24		6,297
GLUL	AI000103	Glutamate-ammonia ligase (glutamine synthase)	Glutamine biosynthesis	1q31		5,576
S100A8	AA086471	S100 calcium binding protein A8 (calgranulin A)	Inflammatory response	1q21		5,485
F2R	AA455910	Coagulation factor II (thrombin) receptor	Apoptosis	5q13		5,352
ASS	AA676466	Argininosuccinate synthetase	Urea cycle	9q34.1		4,978
SH3BGR	N52254	SH3 domain binding glutamic acid-rich protein	SH3/SH2 adaptor protein	21q22.3		4,776
ZFP36	R38383	Zinc finger protein 36, C3H type, homolog (mouse)	mRNA catabolism	19q13.1		4,173
Unknown						
CA3	AA481780	Carbonic anhydrase III, muscle specific	Unknown	8q13-q22	14,648	
TONDU	AA700322	TONDU	Unknown	Xq26.3	12,094	
HRASLS3	AA476438	HRAS-like suppressor 3	Unknown	11q13.1	10,958	
MACMARCK	AA961735	Macrophage myristoylated alanine-rich C kinase substrate	Unknown	1p34.3	8,465	
PROML1	R40057	Prominin-like 1 (mouse)	Unknown	4p15.33	7,650	
EST	H08561	EST	Unknown	2	5,186	
BENE	AA778392	BENE protein	Unknown	2q13	4,832	
EPB41L1	R71689	Erythrocyte membrane protein band 4.1-like 1	Unknown	20q11.2-q12	4,311	
H11	H57494	Protein kinase H11	Unknown	12q24.23	4,229	
sprII		Human small proline rich protein (sprII) mRNA, clone 930	Unknown	Unknown		18,804
EST	AA680300	EST	Unknown	Unknown		7,975
EST	T69164	EST	Unknown	Unknown		7,506
FAT2	H10939	FAT tumor suppressor homolog 2 (Drosophila)	Unknown	5q32-q33		8,997
T1A-2	AA046430	Lung type-I cell membrane-associated glycoprotein	Unknown	1p36		7,024
LIV-1	H29315	LIV-1 protein, estrogen regulated	Unknown	18q12.1		5,927
IGFBP2	H79047	Insulin-like growth factor binding protein 2, 36 kDa	Unknown	2q33-q34		5,441
NCK1	AA280214	NCK adaptor protein 1	Unknown	3q21		4,761
EST	H11482	EST	Unknown	Unknown		4,357
JAG1	R70685	Jagged 1 (Alagille syndrome)	Unknown	20p12.1-p11.23		4,122
EST	AA490044	EST	Unknown	Unknown		4,113

[a]The genes are ranked by mean fold change between Type I and Type II HBECs. The accession numbers are those supplied by SOURCE. [b]GenBank accession number. [c]Gene functions were summarized from literature sources or according to LocusLink in SOURCE or NCBI. [d]Genes are organized according to expression: overexpression from greatest to least followed by fold changes of a ≥4-fold differences in signal intensity between Type I and Type II HBECs. GEV indicates the average of the two biological replicates according to the criteria described in Materials and methods. [e]Genes that have been verified by RT-PCR.

Table III. Up-regulated genes at the immortalization of Type I HBECs.

Functional class	Accession no.[a]	Gene description	Function[b]	Chromosome location	GEV[c]
Extracellular matrix					
FN1	AA489587	Fibronectin 1	Cell adhesion	2q34	7,613
HTF9C	R40127	HpaII tiny fragments locus 9C	ECM composition	22q11.1	4,435
MCAM	AA497002	Melanoma cell adhesion molecule	Cell adhesion	11q23.3	7,513
PNN	W86182	Pinin, desmosome associated protein	Cell adhesion	14q13.2	3,463
Cell cycle					
CCT7	AA676588	Chaperonin containing TCP1, subunit 7 (eta)	Regulation of cell cycle	2p12	3,168
BCL3	AA496678	B-cell CLL/lymphoma 3	Regulation of cell cycle	19q13.1-q13.2	3,163
Cell shape and motility					
ACTG2	T60048	Actin, gamma 2, smooth muscle, enteric	Structural protein of muscle	2p13.1	5,461
ERO1L	AA186804	ERO1-like (S. cerevisiae)	Protein folding	14q22.1	3,079
CCT3	AW075457	Chaperonin containing TCP1, subunit 3 (gamma)	Protein folding	1q23	3,004
TUBA2	AA426374	Tubulin, alpha 2	Cytoskeletal structural protein	13q11	2,753
CCT4	AA598637	Chaperonin containing TCP1, subunit 4 (delta)	Protein folding	2p14	2,749
TUBB4	AW078724	Tubulin, beta, 4	Cytoskeletal structural protein	16q24.3	2,523
Development and differentiation					
THBS1	AA464532	Thrombospondin 1	Development, neurogenesis	15q15	5,720
GSTP1	R33642	Glutathione S-transferase pi	Central nervous system development	11q13	2,492
DNA repair					
ADPRT	H09924	ADP-ribosyltransferase (NAD+; poly (ADP-ribose) polymerase)	DNA repair	1q41-q42	7,838
PCNA	AA450265	Proliferating cell nuclear antigen	DNA repair	20pter-p12	4,268
FEN1	AA620553	Flap structure-specific endonuclease 1	DNA repair	11q12	2,843
Growth					
TPD52L2	R06254	Tumor protein D52-like 2	Cell proliferation	20q13.2-q13.3	2,916
PHB	AA055656	Prohibitin	Negative regulator of cell proliferation	17q21	2,896
MRGX	AA676604	MORF-related gene X	Growth regulation	Xq22	2,838
PRDX1	AA775803	Peroxiredoxin 1	Cell proliferation	1p34.1	2,544
SLC3A2	AA630794	Solute carrier family 3, member 2	Cell growth	11q13	2,409
RBBP4	AA428365	Retinoblastoma binding protein 4	Negative regulation of cell proliferation	1p34.3	2,079
Immune					
CTSC	AA644088	Cathepsin C	Immune response	11q14.1-q14.3	2,990
CNIH	AA521110	Cornichon homolog (Drosophila)	Immune response	14q22.1	2,980
Metabolism					
ENO3	AI963539	Enolase 3, (beta, muscle)	Glycolysis	17pter-p11	3,833
SLC7A5	AA419177	Solute carrier family 7, member 5	Amino acid metabolism	16q24.3	3,656
ODC1	AA461467	Ornithine decarboxylase 1	Polyamine biosynthesis	2p25	3,649
CYC1	AA447774	Cytochrome c-1	Respiratory chain	8q24.3	2,989
ACAT2	R46821	Acetyl-Coenzyme A acetyltransferase 2	Lipid metabolism	6q25.3-q26	2,554
ENO1	AI001174	Enolase 1, (alpha)	Glycolysis	1p36.3-p36.2	2,318
GPI	AA401111	Glucose phosphate isomerase	Carbohydrate metabolism	19q13.1	2,252
Protein synthesis					
EIF2S1	AA669452	eukaryotic translation initiation factor 2, subunit 1 alpha, 35 kDa	Translation initiation factor	14q23.3	5,494
EIF5A	H99842	Eukaryotic translation initiation factor 5A	Regulation of translational initiation	17p13-p12	2,877
KARS	AA486220	Lysyl-tRNA synthetase	Protein biosynthesis	16q23-q24	2,546
RNA processing					
NCL	AA476294	Nucleolin	RNA binding	2q12-qter	3,320
FBL	AA663986	Fibrillarin	rRNA processing	19q13.1	3,085
SNRPN	T54926	Small nuclear ribonucleoprotein polypeptide N	mRNA splicing	15q12	3,051
NOL5A	AA894577	Nucleolar protein 5A (56 kDa with KKE/D repeat)	rRNA processing	20p13	2,605
PABPC1	AA486531	Poly(A) binding protein, cytoplasmic 1	mRNA metabolism	8q22.2-q23	2,542
Transcription					
MYBL2[d]	AA457034	V-myb myeloblastosis viral oncogene homolog (avian)-like 2	Transcription factor	20q13.1	8,091
MRG15	AI979199	MORF-related gene 15	Transcription factor	15q24	3,158
PTTG1	AA430032	Pituitary tumor-transforming 1	Transcription factor	5q35.1	2,712
POLR2J	AA460830	Polymerase (RNA) II (DNA directed) polypeptide J, 13.3 kDa	Transcription from Pol II promoter	7q11.2	2,625
Signaling					
YWHAE	N21624	Tyrosine 3-monooxygenase/tryptophan 5-monooxygenase activation protein, epsilon polypeptide	Intracellular signaling cascade	17p13.3	3,494
TEBP	AA669341	Unactive progesterone receptor, 23 kDa	Signal transduction	12	3,134
STMN1	AA873060	Stathmin 1/oncoprotein 18	Signal transduction	1p36.1-p35	2,986
PIK3R1	R45961	Phosphoinositide-3-kinase, regulatory subunit, polypeptide 1(p85 alpha)	Signal transduction	5q12-q13	2,822
ANXA7	H15446	Annexin A7	Calcium-dependent phospholipid binding	10q21.1-q21.2	2,402
Stress					
HSPD1	AW004895	Heat shock 60 kDa protein 1 (chaperonin)	Stress response	12q12	2,493
HSPE1	AA448396	Heat shock 10 kDa protein 1 (chaperonin 10)	Stress response	2q33.1	2,239
Transport					
SMT3H2	AA775415	SMT3 suppressor of mif two 3 homolog 2 (yeast)	Nucleocytoplasmic transport	17q25.3	2,524
SLC38A2	AA598996	Solute carrier family 38, member 2	Amino acid transport	12q	2,305
Miscellaneous					
UCHL1[d]	AA670438	Ubiquitin carboxyl-terminal esterase L1	Ubiquitin-dependent protein catabolism	4p14	35,651
RAD21	AA683102	RAD21 homolog (S. pombe)	DNA recombination	8q24	4,556
EFEMP1	AA875933	EGF-containing fibulin-like extracellular matrix protein 1	Vision	2p16	4,236
MCM7	AA496025	MCM7 minichromosome maintenance deficient 7 (S. cerevisiae)	DNA replication	7q21.3-q22.1	3,718
CAV1	AA055835	Caveolin 1, caveolae protein, 22 kDa	Tumor suppressor	7q31.1	3,476
IDI1	H08820	Isopentenyl-diphosphate delta isomerase	Isoprenoid biosynthesis	10p15.3	3,309
PSMA3	AA465237	Proteasome (prosome, macropain) subunit, alpha type, 3	Multicatalytic proteinase complex	14q23	3,283
H2AFZ	AI668800	H2A histone family, member Z	Compaction of DNA into nucleosomes	4q24	3,221
EST	AA281733	EST	Nucleosome formation	Unknown	2,104
STOML2	AW075647	Stomatin (EPB72)-like 2	Receptor binding	9p13.1	2,080
Unknown					
EST	AA427899	Homo sapiens clone 24464 beta-tubulin mRNA, complete cds	Unknown	Unknown	12,657
C14orf3	AA411202	Chromosome 14 open reading frame 3	Unknown	14q23.3-31	3,615
FLJ22678	N90109	Hypothetical protein FLJ22678	Unknown	2q36.3	3,272
EST	AA115309	ESTs, Highly similar to 2209333A protein disulfide isomerase	Unknown	Unknown	2,859

[a]GenBank accession number. [b]Gene functions were summarized from literature sources or according to LocusLink in SOURCE or NCBI. [c]Genes are organized according to expression: up-regulation from greatest to least followed by fold changes of a ≥2-fold differences in signal intensity between Type I HBECs and M13SV1. GEV indicates the average of the two biological replicates according to the criteria described in Materials and methods. [d]Genes that have been verified by RT-PCR.

Table IV. Down-regulated genes at the immortalization of Type I HBECs.

Functional class	Accession no.[a]	Gene description	Function[b]	Chromosome location	GEV[c]
Extracellular matrix					
MMP7	AA031514	Matrix metalloproteinase 7 (matrilysin, uterine)	Proteolysis and peptidolysis	11q21-q22	-133,333
LAMC2	AA677534	Laminin, gamma 2	Cell adhesion	1q25-q31	-8,850
LAMB3	AW007267	Laminin, beta 3	Cell adhesion	1q32	-7,752
COL4A2	AA430540	Collagen, type IV, alpha 2	ECM composition	13q34	-5,698
TNC	R39239	Tenascin C (hexabrachion)	Cell adhesion	9q33	-17,094
CD151	AA443118	CD151 antigen	Cell adhesion	11p15.5	-8,230
GPR56	AA775249	G protein-coupled receptor 56	Cell adhesion	16q13	-5,168
NK4	AA458965	Natural killer cell transcript 4	Cell adhesion	16p13.3	-3,854
AGRN	AA458878	Agrin	Component of the basal lamina	1p36.3-p32	-2,193
Cell cycle					
SNK	AA460152	Serum-inducible kinase	Regulation of cell cycle progression	5q12.1-q13.2	-13,245
CCND1	AA487486	Cyclin D1 (PRAD1: parathyroid adenomatosis 1)	G1/S regulation	11q13	-7,843
QSCN6	AA464152	Quiescin Q6	Regulation of cell cycle	1q24	-3,145
CCNI	AA434408	Cyclin I	Cell cycle regulation	4q13.3	-2,751
CDK2AP1	R78607	CDK2-associated protein 1	DNA replication during S phase	12q24.31	-2,538
CDKN1A	AI952615	Cyclin-dependent kinase inhibitor 1A (p21, Cip1)	Cell cycle arrest	6p21.2	-2,195
Cell shape and motility					
CRYAB	AA504891	Crystallin, alpha B	Protein folding	11q22.3-q23.1	-32,787
CTGF	AA598794	Connective tissue growth factor	Cell motility	6q23.1	-10,638
GSN	H72028	Gelsolin (amyloidosis, Finnish type)	Actin modification	9q33	-8,439
KRT19	AA464250	Keratin 19	Intermediate filaments	17q21.2	-7,353
MYH9	T69926	Myosin, heavy polypeptide 9, non-muscle	Cell shape	22q13.1	-4,237
MYL9	AA877166	Myosin, light polypeptide 9, regulatory	Structural protein of muscle	20q11.22	-4,228
MYOC	AI971049	Myocilin	Cytoskeleton	1q23-q24	-3,906
EST	N93021	EST	Tubulin folding	Unknown	-2,584
MARCKS	AA482231	Myristoylated alanine-rich protein kinase C substrate	Cell motility	6q22.2	-2,413
Development and differentiation					
KLK7	AI139437	Kallikrein 7 (chymotryptic, stratum corneum)	Epidermal differentiation	19q13.41	-62,500
TAGLN	AI668906	Transgelin	Muscle development	11q23.2	-12,739
KLK5	W73140	Kallikrein 5	Epidermal differentiation	19q13.3-q13.4	-9,259
EMP1	AA975768	Epithelial membrane protein 1	Epidermal differentiation	12p12.3	-4,608
JWA	AA489479	Vitamin A responsive; cytoskeleton related	Regulation of cell differentiation	3p14	-3,752
KRT14	H44051	Keratin 14 (epidermolysis bullosa simplex)	Epidermal differentiation	17q12-q21	-2,899
KRT5	AA160507	Keratin 5 (epidermolysis bullosa simplex)	Epidermal differentiation	12q12-q13	-2,710
FN14	AI221536	Type I transmembrane protein Fn14	Development	16p13.3	-2,255
Growth					
RARRES1	N94424	Retinoic acid receptor responder (tazarotene induced) 1	Negative regulation of cell proliferation	3q25.31	-47,619
BTG1	N70463	B-cell translocation gene 1, anti-proliferative	Negative regulation of cell proliferation	12q22	-6,135
TPT1	AI671926	Tumor protein, translationally-controlled 1	Cell growth	13q12-q14	-3,846
CYR61	AA777187	Cysteine-rich, angiogenic inducer, 61	Cell proliferation	1p31-p22	-3,766
S100A11	AA464731	S100 calcium binding protein A11 (calgizzarin)	Negative regulation of cell proliferation	1q21	-2,660
Immune					
F3	AI313387	Coagulation factor III (thromboplastin, tissue factor)	Immune response	1p22-p21	-21,277
CD24	H59916	CD24 antigen (small cell lung carcinoma cluster 4 antigen)	Humoral immune reponse	6q21	-14,184
CD59	H60549	CD59 antigen p18-20	Immune response	11p13	-4,301
HLA-C	AA464246	Major histocompatibility complex, class I, C	Immune response	6p21.3	-3,831
HLA-B	AW082023	Major histocompatibility complex, class I, B	Immune response -	6p21.3	-3,236
HLA-DOA	AA702254	Major histocompatibility complex, class II, DO alpha	Immune response	6p21.3	-2,700
HLA-A	AA644657	Major histocompatibility complex, class I, A	Immune response	6p21.3	-2,677
Metabolism					
ALDH1A3	AA455235	Aldehyde dehydrogenase 1 family, member A3	Lipid metabolism	15q26.3	-8,873
UQCR	AA629862	Ubiquinol-cytochrome c reductase (6.4 kDa) subunit	Mitochondrial respiratory chain	19p13.3	-4,515
CDA	AA922903	Cytidine deaminase	Nucleotide and nucleic acid metabolism	1p36.2-p35	-3,968
SDR1	AA171606	Short-chain dehydrogenase/reductase 1	Fatty acid metabolism	1p36.1	-3,565
FDFT1	AA679352	Farnesyl-diphosphate farnesyltransferase 1	Steroid biosynthesis	8p23.1-p22	-2,315
Transcription					
MEF2C	AA234897	MADS box transcription enhancer factor 2, polypeptide C	Transcription factor	5q14	-5,865
ELF3	AA434373	E74-like factor 3	Transcription factor	1q32.2	-3,413
ZFP36L1	AA424743	Zinc finger protein 36, C3H type-like 1	Transcription factor	14q22-q24	-2,392
Signal					
IGFBP3	AA598601	Insulin-like growth factor binding protein 3	Signal transduction	7p13-p12	-13,158
CD81	AA486556	CD81 antigen (target of antiproliferative antibody 1)	Signal transduction	11p15.5	-7,067
SE20-4	AI969825	Cutaneous T-cell lymphoma-associated tumor antigen se20-4	Signal transduction	7	-3,322
ANXA3	AI949576	Annexin A3	Signal transduction	4q13-q22	-3,241
CRABP2	AA598508	Cellular retinoic acid binding protein 2	Signal transduction	1q21.3	-3,210
INHBA	N27159	Inhibin, beta A (activin A, activin AB alpha polypeptide)	Signal transduction	7p15-p13	-3,091
TGFBR2	AA487034	Transforming growth factor, beta receptor II (70/80 kDa)	Signal transduction	3p22	-2,959
AKT1	AA464217	V-akt murine thymoma viral oncogene homolog 1	Serine-threonine protein kinase	14q32.32	-2,954
TNFRSF1A	W02761	Tumor necrosis factor receptor superfamily, member 1A	Signal transduction	12p13.2	-2,920
MLP	AA961735	MARCKS-like protein	Signal transduction	1p34.3	-2,911
RAI3	AA172400	Retinoic acid induced 3	Signal transduction	12p13-p12.3	-2,736
PTPRF	AA598513	Protein tyrosine phosphatase, receptor type, F	Signal pathway	1p34	-2,281
ANXA8	AA235002	Annexin A8	Signal transduction	10q11.2	-2,039
Miscellaneous					
SERPINA3	AA704242	Serine (or cysteine) proteinase inhibitor, clade A, member 3	Acute-phase response	14q32.1	-133,333
LCN2	AA400973	Lipocalin 2 (oncogene 24p3)	Transport of small lipophilic substances	9q34	-20,619
FHL2	AA995282	Four and a half LIM domains 2	Oncogenesis	2q12-q14	-5,155
MGC20576	H51645	Hypothetical protein MGC20576	Non-lysosomal thiol-protease	19q13.2	-5,000
SDC4	AA148737	Syndecan 4 (amphiglycan, ryudocan)	Cell surface proteoglycan	20q12	-4,587
LGALS1	AI927284	Lectin, galactoside-binding, soluble, 1 (galectin 1)	Apoptosis	22q13.1	-3,831
TNIP1	T64483	TNFAIP3 interacting protein 1	Defense response	5q32-q33.1	-3,745
PIG3	AA668595	Quinone oxidoreductase homolog	Oxidative stresses and irradiation	2p23.3	-3,322
H2AFY	AA488627	H2A histone family, member Y	Nucleosome modeling	5q31.3-q32	-3,067
CLIC4	AA634261	Chloride intracellular channel 4	Chloride channel	1p36.11	-3,003
NPC2	AA630449	Niemann-Pick disease, type C2	Reproduction	14q24.3	-2,475
RPL29	AW073449	Ribosomal protein L29	RNA binding	3p21.3-p21.2	-2,421
CD9	AA412053	CD9 antigen (p24)	Platelet activation and aggregation	12p13.3	-2,172
Unknown					
EST	AA634103	Human promyelocytic leukemia cell mRNA	Unknown	Unknown	-5,376
EST	AA629897	EST	Unknown	Unknown	-4,773
MGC5618	AA488084	hypothetical protein MGC5618	Unknown	Unknown	-2,920

[a]GenBank accession number. [b]Gene functions were summarized from literature sources or according to LocusLink in SOURCE or NCBI. [c]Genes are organized according to expression: down-regulation from greatest to least followed by fold changes of a ≥2-fold differences in signal intensity between Type I HBECs and MI3SV1. GEV indicates the average of the two biological replicates according to the criteria described in Materials and methods. [d]Genes that have been verified by RT-PCR.
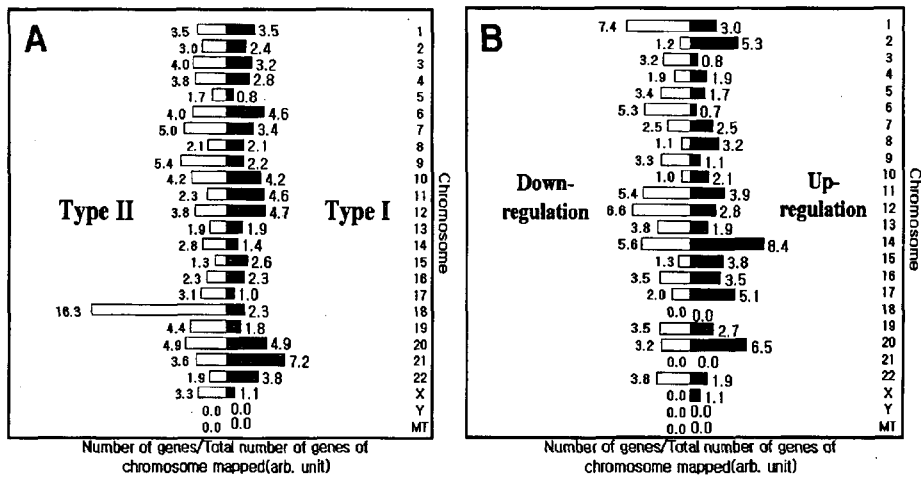
Figure 3. Chromosomal locations in normal HBECs and immortal HBECs. (A), Two types of HBECs. (B), Immortalized HBEC line derived from Type I HBECs. The x-axis indicates how many changed genes map to each chromosome, and the y-axis refers to the set of human chromosomes. Since mapping information was obtained from LocusLink (NCBI), values on the x-axis were normalized for each chromosome to the total number of genes/chromosome mapped in LocusLink.

from normal HBECs with luminal cell properties using cDNA microarray. The phenotype of Type I HBECs is suggestive of the presence of stem cells in the Type I HBEC population, as some of them have the ability to give rise to another type of cells with a different phenotype, i.e. Type I HBECs (expressing luminal epithelial cell markers) to Type II HBECs (expressing basal epithelial cell markers) (3). In addition, Type I HBECs are deficient in GJIC: GJIC deficiency has been reported to be a characteristic of putative stem cells (3,10,12-15). More recently, a number of groups have claimed to have isolated mammary stem cells (30-34). In addition, it has been shown that there exists a human breast cancer stem cell (35,36).

Importantly, these two normal breast epithelial types of cells were different substantially in their response to an oncogenic (SV40) stimulus; i.e., Type I HBECs were AIG+, whereas SV40-transformed Type II cells totally lack the ability to grow in soft agar (AIG) (3). Therefore, Type I HBECs are more susceptible to tumorigenic initiation by acquiring two major and common tumor cell phenotypes, i.e., AIG+ and immortality. Both normal Type I and Type II HBECs had a low level of telomerase activity that was insufficient to maintain continuous cell proliferation unless it was activated and the high potential of telomerase activation for Type I HBECs resulted in a more efficient immortalization compared to Type II HBECs (4). Because Type I HBECs have stem cell characteristics, these results suggest that the aforementioned mechanism is the reason why stem cells are more likely to be target cells for neoplastic transformation.

The differential expression pattern and the function of several candidate genes detected by cDNA microarray are consistent with those reported for various human breast epithelial cells (3-5,7,11,15,16,37).

The differentially expressed genes identified between Type I and II HBECs are mainly related with signal transduction, cell adhesion, immune response, metabolism and cell proliferation. ITGA6, one of basal epithelial cell markers, were found to be highly expressed in Type II HBECs. A member of the matrix metalloproteinase family, MMP7 was highly expressed in Type I HBECs, but not in Type II HBECs. Especially, several collagen genes are involved in ECM assembly that form basement membranes, COL1A2 is highly expressed in Type I HBECs and COL7A1 in Type II. Two major components of microtubules, K-ALPHA-1 and TUBB, are more highly expressed in Type I HBECs than in Type II HBECs. CTGF is overexpressed in Type I HBECs. Cyclin D1 is likely to reveal core stem cell properties or 'stemness' that underlie self-renewal and the ability to generate differentiated progeny (38). As expected, the expression of Cyclin D1 is found to be higher in Type I HBECs than in Type II cells. Keratin 19 is more expressed approximately 1.5-fold in Type I HBECs than in Type II HBECs (data not shown). Previously, a subpopulation of luminal epithelial cells in the normal breast in situ by the restricted expression of Keratin 19 was localized (16). Keratin 19 is one of the earliest keratin expressed in the embryo (39), and whereas the fetal breast contains a homogeneously keratin 19+ luminal epithelial compartment, keratin 19- luminal cells arise only in adulthood (40). Expectedly, gap junction binding 2 (GJB2) gene encoding connexin-26, a GJIC protein, is found to be highly expressed in Type II HBECs, but little expression of it in Type II HBECs and M13SV1 (data not shown). This result is consistent with our pervious data. Dysfunction of gap junctional intercellular communication has been linked to teratogenesis, carcinogenesis, specifically the tumor promotion and progression phases, reproductive dysfunction, neurological anomalies and many other disease states (41).

MME, an important cell surface marker in the diagnosis of human acute lymphocytic leukemia (ALL), is highly expressed in Type II HBECs. The common acute lymphoblastic leukemia antigen (*CALLA/CD10/neutral endopeptidase 24.11*) was used to mark the myoepithelial cells (42). *Tumor protein p63* is a gene implicated in regulating normal epithelial development and differentiation and is a characterized p53-homolog that is consistently expressed by basal/somatic stem cells of stratified epithelia, myoepithelial cells of the breast and salivary glands, and proliferative compartment of gastric mucosa (43). Especially, The *p63* overexpressed in Type II HBECs is consistant with these studies. *Cathepsin C, D, L and L2* (data not shown), *Cystatin A, Serine (or cysteine) proteinase inhibitor, clade B, member 3* and *member 5 (maspin), S100 calcium-binding protein A8* is highly expressed in Type II HBECs. But, *Cathepsin H* (data not shown) is highly expressed in Type I HBECs. p63, protease, Cathepsin D, maspin, S-100 calcium-binding protein A8 are novel putative marker protein of myoepithelial cells (44,45). Therefore, *Cathepsin C, L and H* also may become the candidate gene or marker capable of classifying human breast cells.

Most of the highly up- or down-related genes between normal and SV40-immortalized HBECs with stem and luminal cell characteristics cover a broad spectrum of cellular processes including cell adhesion, cell cycle, signal transcription, and cell proliferation. In bypassing senescence, Type I HBECs appear to lose many specialized functions associated with proliferating, mortal HBECs. Of 81 genes down-regulated upon immortalization, ~20 are associated with an epithelial cell function. For example, SV40-immortalized Type I HBECs lose expression of epithelial cell-specific *kallikrein 5 (KLK5)* and *7 (KLK7)*, two serine proteases potentially important in tumor growth (46,47). *Connective tissue growth factor (CTGF)* is down-regulated in M13SV1. Accordingly, this fact is consistent with non-tumorigenic property of M13SV1. *Gelsolin (GSN)* and *Keratin 19 (KRT19)* are less expressed in M13SV1. GSN, a multifunctional actin-binding protein, plays a critical role in regulating the dynamic changes in the actin cytoskeleton. Deregulation of GSN apparently occurs early in tumorigenesis (48). Microarray analysis shows that *TAGLN, KLK7, EMP1* and *RARRES1* are down-regulated in M13SV1. TAGLN is identified previously as a transformation and shape change-sensitive actin-gelling protein whose expression was lost in virally transformed cell lines (49). Ras-dependent and Ras-independent mechanisms can cause the down-regulation of TAGLN in human breast and colon carcinoma cell lines and patient-derived tumor samples. Therefore, loss of *TAGLN* gene expression might be an important early event in tumor progression and a diagnostic marker for breast and colon cancer development (49). EMP1 (TMP, CL20 and B4B) is a members of the PMP22/EMP/MP20 family of membrane glycoproteins, in squamous cell differentiation (50,51). Its precise functions in the breast are unknown but associations with cell proliferation and tumorigenesis have been proposed, differential expression of it has been reported in estrogen-resistant MCF7ADR breast cancer cells (52) and its down-regulation was linked to induction of G1 arrest (53).

The expression of *cyclin D1 (CCND1)* is lower in M13SV1 than in Type I HBECs, which is consistent with previous results at the protein level (5). In our data, the immortalization of Type I HBECs results in additional changes to the cyclin D1-dependent cell cycle regulatory pathways such as down-regulation of *cyclin D1, cdk6*, and up-regulation of *cyclin A2, cyclin B2, cyclin E2, cdk2, PCNA* (data not shown). Concurrent deregulation of GSN and cyclin D1 is highly prevalent among breast cancers of humans and rodents (54).

Not surprisingly, immortalized Type I HBECs activate or inactivate genes that participate in pathways that promote proliferation, including transcription factor and signal proteins. In addition, genes involved in DNA repair response were also up-regulated during immortalization. Transcript levels of negative growth regulators were decreased including the p53-regulated targets cyclin-dependent kinase inhibitor 1A (CDKN1A) and insulin-like growth factor binding protein 3 (IGFBP3) (Table IV), suggesting declined p53 activity for immortalization. p21, a cyclin-dependent kinase inhibitor and a marker of cellular senescence, disappeared in the life span-extended cells by T antigen. IGFBP3 has been demonstrated to be an important mediator of other growth inhibitory agents, such as retinoic acid (55), vitamin D (56), TGF-ß, (57), anti-estrogens (58), tumor necrosis factor-α (59) and p53 (60), independently of the IGF signaling system. *Transforming growth factor, beta receptor II (TGFBR2)* was also repressed in immortalized cells. IGFBP-3 antiproliferative signalling appears to require an active transforming growth factor beta (TGF-ß) signaling pathway. In some epithelial cancer cells, the growth inhibitory effect of TGF-ß on cell growth has been shown to be mediated by the up-regulation of IGFBP-3 mRNA and protein levels (61,62). A signaling pathway through which IGFBP-3 action is mediated from the activation of a cell surface receptor to the induction of gene transcription in the nucleus had been identified (63). This pathway requires the presence of TGF-ßRII. Exactly how IGFBP-3 initiates this pathway is an important unanswered question. *V-myb myeloblastosis viral oncogene homolog (avian)-like 2 (MYBL2)* and *ubiquitin carboxyl-terminal esterase L1 (UCHL1)* are highly expressed in M13SV1. The *MYBL2 (B-myb)* gene belongs to the MYB family of transcription factor genes and plays an essential role during cell cycle progression. MYBL2 transcripts are detectable in a wide variety of dividing cell types. MYBL2 can stimulate expression of the *UCHL1* (64).

Lipocalin 2 (LCN2), a component of the neutrophil gelatinase complex, is found to be highly expressed in Type I HBECs, but is shown to be significantly repressed in M13SV1. It is a putative *in vivo* estrogen target gene and candidate paracrine factor that might mediate estrogen-induced proliferation in the normal breast epithelium (65). These results demonstrate that normal and cancerous estrogen receptor-positive cells are distinct at the molecular level and suggest that *LCN2* is a new therapeutic target for breast cancer prevention and treatment (65).

According to our microarray analyses, Type I HBECs express genes involved in luminal cell and stem cell characteristics (e.g., *Keratin 19, Cyclin D1*, etc.), while Type II HBECs express genes related in basal and/or myo-epithelial cell (e.g., *integrin alpha 6, connexin 26, CALLA, p63, cathepsin D*, and *maspin*, etc.). We have identified genes participating in normal human breast luminal epithelial

cell immortalization. We suspect that these genes are members of a limited number of pathways that can be inactivated to bypass senescence during tumorigenesis (66). cDNA micro-array can be a powerful approach method of defining putative amplification target genes such as comparative genomic hybridization (CGH). A cDNA microarray analysis was performed to study the relationship of gene expression and genomic copy number (67). As biological processes can be regulated within a local chromosomal region (e.g., imprinting), an additional profile is constructed for the chromosome location. The evidence that the chromosome 21 has the most of genes overexpressed in Type I compared to Type II HBECs, indicates that many stem cell-related genes might reside on the chromosomal locus. Ten of up-regulated genes are on chromosome 14, which means that this chromosome contains several times immortalized Type I HBEC-enriched genes than would be present if these genes were randomly distributed. It is possible that some of the clustered Type I HBEC-enriched genes are co-regulated at a local chromatin level and their proximity in the genome might reflect an ancestral clustering of stem cell genes.

These observations support the hypothesis that the origin of human breast carcinomas could be the luminal epithelial cell or its precursor cell and suggest that the Type I HBECs described in this communication might be the major target cells for neoplastic transformation (3). Cancer cells are believed to arise from stem cells or early precursor cells and often have a phenotype similar to normal undifferentiated cells (68) or have a combined phenotype of different cell types of a common lineage (e.g. leukemia cells often express both lymphoid and myeloid cell antigens). Therefore, cancer has been termed a disease of the pluripotent stem cell (69), a disease of cell differentiation (70) or 'oncogeny as blocked or partially blocked ontogeny' (18). As a possible challenge to the prevailing paradigm that the first step of carcinogenesis is the immortalization of a normal 'mortal' cell and followed by the neoplastic transformation of this 'immortalized' cell, these data suggest that the normal mammary stem cell, which is naturally immortal by nature, is blocked from 'mortalization' during the first step of carcinogenesis and then neoplastically transformed. In this manner, the cancer cell would share many phenotypic markers expressed in both the normal stem cell and the 'immortalized' or 'blocked mortalized' cell.

Taken together, our microarray data indicate that Type I HBECs and/or M13SV1-enriched genes might be normal human breast epithelial stem cell-related genes. This study does not indicate only that Type I HBECs might contain both stem cells and luminal epithelial cells, but that M13SV1 might be one of in vitro model concerning the mechanism of carcinogenic initiation of breast epithelial cells. Consequently, the investigation of gene expression changes associated with SV40 in normal HBECs and M13SV1 cell line could be very valuable to stem cell and tumor biologists. We propose that candidate stem cells of the human breast should be found within the Type I HBEC populations, that these cells isolated and characterized should fulfill the criteria for such candidate stem cells, and that further study on those new genes manifested by cDNA microarray might throw light on the understanding of breast carcinogenesis.

Acknowledgments

References

1. Bartek J, Durban EM, Hallowes RC and Taylor-Papadimitriou J: A subclass of luminal epithelial cells in the human mammary gland, defined by antibodies to cytokeratins. J Cell Sci 75: 17-33, 1985.
2. Taylor-Papadimitriou J, Stampfer M, Bartek J, Lewis A, Boshell M, Lane EB and Leigh IM: Keratin expression in human mammary epithelial cells cultured from normal and malignant tissue: relation to in vivo phenotypes and influence of medium. J Cell Sci 94: 403-413, 1989.
3. Kao CY, Nomata K, Oakley CS, Welsch CW and Chang CC: Two types of normal human breast epithelial cells derived from reduction mammoplasty: phenotypic characterization and response to SV40 transfection. Carcinogenesis 16: 531-538, 1995.
4. Sun W, Kang KS, Morita I, Trosko JE and Chang CC: High susceptibility of a human breast epithelial cell type with stem cell characteristics to telomerase activation and immortalization. Cancer Res 59: 6118-6123, 1999.
5. Kang KS, Morita I, Cruz A, Jeon YJ, Trosko JE and Chang CC: Expression of estrogen receptors in a normal human breast epithelial cell type with luminal and stem cell characteristics and its neoplastically transformed cell lines. Carcinogenesis 18: 251-257, 1997.
6. Kang KS, Sun W, Nomata K, Morita I, Cruz A, Liu CJ, Trosko JE and Chang CC: Involvement of tyrosine phosphorylation of p185(c-erbB2/neu) in tumorigenicity induced by X-rays and the neu oncogene in human breast epithelial cells. Mol Carcinog 21: 225-233, 1998.
7. Kang KS, Chang CC and Trosko JE: Modulation of gap junctional intercellular communication during human breast stem cell differentiation and immortalization. In: Gap Junctions. Werner R (ed.) IOS Press, Amsterdam, pp347-351, 1998.
8. Williams JM and Daniel CW: Mammary ductal elongation: differentiation of myoepithelium and basal lamina during branching morphogenesis. Dev Biol 97: 274-290, 1983.
9. Monaghan P, Perusinghe NP, Cowen P and Gusterson BA: Peripubertal human breast development. Anat Rec 226: 501-508, 1990.
10. Trosko JE, Chang CC, Wilson MR, Upham B, Hayashi T and Wade M: Gap junctions and the regulation of cellular functions of stem cells during development and differentiation. Methods 20: 245-264, 2000.
11. Stingl J, Eaves CJ, Kuusk U and Emerman JT: Phenotypic and functional characterization in vitro of a multipotent epithelial cell present in the normal adult human breast. Differentiation 63: 201-213, 1998.
12. Chang CC, Trosko JE, El-Fouly MH, Gibson-D'Ambrosio RE and D'Ambrosio SM: Contact insensitivity of a subpopulation of normal human fetal kidney epithelial cells and of human carcinoma cell lines. Cancer Res 47: 1634-1645, 1987.
13. Matic M, Petrov IN, Chen S, Wang C, Dimitrijevich SD and Wolosin JM: Stem cells of the corneal epithelium lack connexins and metabolite transfer capacity. Differentiation 61: 251-260, 1997.
14. Matic M, Evans WH, Brink PR and Simon M: Epidermal stem cells do not communicate through gap junctions. J Invest Dermat 118: 110-116, 2002.
15. Trosko JE: The role of stem cells and gap junctional intercellular communication in carcinogenesis. J Biochem Mol Biol 36: 43-48, 2003.
16. Gudjonsson T, Villadsen R, Nielsen HL, Ronnov-Jessen L, Bissell MJ and Petersen OW: Isolation, immortalization, and characterization of a human breast epithelial cell line with stem cell properties. Genes Dev 16: 693-706, 2002.
17. Trosko JE and Chang CC: Role of stem cells and gap junctional intercellular communication in human carcinogenesis. Radiat Res 155: 175-180, 2000.
18. Potter VR: Phenotypic diversity in experimental hepatomas: the concept of partially blocked ontogeny. The 10th Walter Hubert Lecture. Br J Cancer 38: 1-23, 1978.

19. Blau HM, Brazelton TR and Weimann JM: The evolving concept of a stem cell: entity or function. Cell 105: 829-841, 2001.
20. Ying QL, Nichols J, Evans EP and Smith AG: Changing potency by spontaneous fusion. Nature 416: 545-548, 2002.
21. Chen H, Campisi J and Padmanabhan R: SV40 large T antigen transactivates the human cdc2 promoter by inducing a CCAAT box binding factor. J Biol Chem 271: 13959-13967, 1996.
22. Kiyono T, Foster SA, Koop JI, McDougall JK, Galloway DA and Klingelhutz AJ: Both Rb/p16INK4a inactivation and telomerase activity are required to immortalize human epithelial cells. Nature 396: 84-88, 1998.
23. Miksicek RJ, Myal Y, Watson PH, Walker C, Murphy LC and Leygue E: Identification of a novel breast- and salivary gland-specific, mucin-like gene strongly expressed in normal and tumor human mammary epithelium. Cancer Res 62: 2736-2740, 2002.
24. Yang SH, Kim JS, Oh TJ, Kim MS, Lee SW, Woo SK, Cho HS, Choi YH, Kim YH, Rha SY, Chung HC and An SW: Genome-scale analysis of resveratrol-induced gene expression profile in human ovarian cancer cells using a cDNA microarray. Int J Oncol 22: 741-750, 2003.
25. Eiesen MB, Spellman PT, Brown PO and Botstein D: Cluster analysis and display of genomic-wide expression patterns. Proc Natl Acad Sci USA 95: 14863-14868, 1998.
26. Schadt EE, Li C, Su C and Wong WH: Analyzing high-density oligonucleotide gene expression array data. J Cell Biochem 80: 192-202, 2000.
27. Ray FA and Kraemer PM: Frequent deletions in nine newly immortal human cell lines. Cancer Genet Cytogenet 59: 39-44, 1992.
28. Banga SS, Kim SH, Hubbard K, Dasgupta T, Jha KK, Patsalis P, Hauptschein R, Gamberi B, Dalla-Favera R, Krarmer P and Ozer HL: SEN6, a locus for SV-40-mediated immortalization of human cells, map to 6q26-27. Oncogene 14: 313-321, 1997.
29. Savelieva E, Belair CD, Newton MA, De Vries S, Gray JW, Waldman F and Reznikoff CA: 20q gain associates with immortalization: 20q13.2 amplication correlates with genome instability in human papilloma virus 16 E7 transformed human uroepithelial cells. Oncogene 14: 551-560, 1997.
30. Smith GH and Boulanger CA: Mammary epithelial stem cells: transplantation and self renewal analysis. Cell Prolif 36: 3-15, 2003.
31. Welm B, Behbod F, Goodell MA and Rosen JM: Isolation and characterization of functional mammary gland stem cells. Cell Prolif 36: 17-32, 2003.
32. Petersen OW, Gudjonsson T and Villadsen R: Epithelial progenitor cell lines as models of normal, breast morphogenesis and neoplasia. Cell Prolif 36: 33-44, 2003.
33. Clarke RB, Anderson E, Howell, and Potten CS: Regulation of human breast epithelial stem cells. Cell Prolif 36: 45-58, 2003.
34. Boecker W and Buerger H: Evidence of projector cells of glandular and myoethelial cell linages in the human adult female breast epithelium: a new progenitor (adult stem cell) cell concept. Cell Prolif 36: 73-84, 2003.
35. Al-Hajj M, Wicha MS, Benito-Hernandez A, Morrison SJ and Clarke MF: Prospective identification of tumorigenic breast cancer cells. Proc Natl Acad Sci USA 100: 3983-3988, 2003.
36. Dick JE: Breast cancer stem cells revealed. Proc Natl Acad Sci USA 100: 3547-3549, 2003.
37. Pechoux C, Gudjonsson T, Ronnov-Jessen L, Bissell MJ and Petersen OW: Human mammary luminal epithelial cells contain progenitors to myoepithelial cells. Dev Biol 206: 88-99, 1999.
38. Ramalho-Santos M, Yoon S, Matsuzaki Y, Mulligan RC and Melton DA: 'Stemness': transcriptional profiling of embryonic and adult stem cells. Science 298: 597-600, 2002.
39. Tamai Y, Ishikawa T, Bosl MR, Mori M, Nozaki M, Baribault H, Oshima RG and Taketo MM: Cytokeratins 8 and 19 in the mouse placental development. J Cell Biol 151: 563-572, 2000.
40. Anbazhagan R, Osin PP, Bartkova J, Nathan B, Lane EB and Gusterson BA: The development of epithelial phenotypes in the human fetal and infant breast. J Pathol 184: 197-206, 1998.
41. Trosko JE, Madhukar BV and Chang CC: Endogenous and exogenous modulation of gap junctional intercellular communication, toxicological and pharmacological implications. Life Sci 53: 1-19, 1993.
42. Gusterson BA, Monaghan P, Mahendran R, Ellis J and O'Hare MJ: Identification of myoepithelial cells in human and rat breasts by anti-common acute lymphoblastic leukemia antigen antibody A12. J Natl Cancer Inst 77: 343-349, 1986.
43. Reis-Filho JS and Schmitt FC: Taking advantage of basic research: p63 is a reliable myoepithelial and stem cell marker. Adv Anat Pathol 9: 280-289, 2002.
44. Li P, Barraclough R, Fernig DG, Smith JA and Rudland PS: Stem cells in breast epithelia. Int J Exp Pathol 79: 193-206, 1998.
45. Reis-Filho JS, Milanezi F, Paredes J, Silva P, Pereira EM, Maeda SA, De Carvalho LV and Schmitt FC: Novel and classic myoepithelial/stem cell markers in metaplastic carcinomas of the breast. Appl Immunohistochem Mol Morphol 11: 1-8, 2003.
46. Tanimoto H, Underwood LJ, Shigemasa K, Yan Yan MS, Clarke J, Parmley TH and O'Brien TJ: The stratum corneum chymotryptic enzyme that mediates shedding and desquamation of skin cells is highly overexpressed in ovarian tumor cells. Cancer 86: 2074-2082, 1999.
47. Kim H, Scorilas A, Katsaros D, Yousef GM, Massobrio M, Fracchioli S, Piccinno R, Gordini G and Diamandis EP: Human kallikrein gene 5 (KLK5) expression is an indicator of poor prognosis in ovarian cancer. Br J Cancer 84: 643-650, 2001.
48. Habeck M: Gelsolin: a new marker for breast cancer? Mol Med Today 5: 503, 1999.
49. Shields JM, Rogers-Graham K and Der CJ: Loss of transgelin in breast and colon tumors and in RIE-1 cells by Ras deregulation of gene expression through Raf-independent pathways. J Biol Chem 277: 9790-9799, 2002.
50. Chen Y, Medvedev A, Ruzanov P, Marvin KW and Jetten AM: cDNA cloning, genomic structure, and chromosome mapping of the human epithelial membrane protein CL-20 gene (EMP1), a member of the PMP22 family. Genomics 41: 40-48, 1997.
51. Ben-Porath I, Yanuka O and Benvenisty N: The tmp gene, encoding a membrane protein, is a c-Myc target with a tumorigenic activity. Mol Cell Biol 19: 3529-3539, 1999.
52. Schiemann S, Ruckels M, Engelholm LH, Schwirzke M, Brunner N and Weidle UH: Differential gene expression in human mammary carcinoma cells: identification of a new member of a receptor family. Anticancer Res 17: 13-20, 1997.
53. Gnirke AU and Weidle UH: Investigation of prevalence and regulation of expression of progression associated protein (PAP). Anticancer Res 18: 4363-4369, 1998.
54. Dong Y, Asch HL, Medina D, Ip C, Ip M, Guzman R and Asch BB: Concurrent deregulation of gelsolin and cyclin D1 in the majority of human and rodent breast cancers. Int J Cancer 81: 930-938, 1999.
55. Gucev ZS, Oh Y, Kelley KM and Rosenfeld RG: Insulin-like growth factor binding protein 3 mediates retinoic acid- and transforming growth factor beta2-induced growth inhibition in human breast cancer cells. Cancer Res 56: 1545-1550, 1996.
56. Colston KW, Perks CM, Xie SP and Holly JM: Growth inhibition of both MCF-7 and Hs578T human breast cancer cell lines by vitamin D analogues is associated with increased expression of insulin-like growth factor binding protein-3. J Mol Endocrinol 20: 157-162, 1998.
57. Oh Y, Müller HL, Lamson G and Rosenfeld RG: Insulin-like growth factor (IGF)-independent action of IGF-binding protein-3 in Hs578T human breast cancer cells. Cell surface binding and growth inhibition. J Biol Chem 268: 14964-14971, 1993.
58. Huynh H, Yang X and Pollak M: A role for insulin-like growth factor binding protein 5 in the antiproliferative action of the antiestrogen ICI 182780. J Biol Chem 271: 1016-1021, 1996.
59. Rozen F, Zhang J and Pollak M: Antiproliferative action of tumor necrosis factor-alpha on MCF-7 breastcancer cells is associated with increased insulin-like growth factor binding protein-3 accumulation. Int J Oncol 13: 865-869, 1998.
60. Buckbinder L, Talbott R, Velasco-Miguel S, Takenaka I, Faha B, Seizinger BR and Kley N: Induction of the growth inhibitor IGF-binding protein 3 by p53. Nature 377: 646-649, 1995.
61. Oh Y, Müller HL, Lamson G and Rosenfeld RG: Transforming growth factor-beta-induced cell growth inhibition in human breast cancer cells is mediated through insulin-like growth factor-binding protein-3 action. J Biol Chem 270: 13589-13592, 1995.
62. Rajah R, Valentinis B and Cohen P: Insulin-like growth factor (IGF)-binding protein-3 induces apoptosis and mediates the effects of transforming growth factor-beta1 on programmed cell death through a p53- and IGF-independent mechanism. J Biol Chem 272: 12181-12188, 1997.

63. Fanayan S, Firth SM and Baxter RC: Signaling through the Smad pathway by insulin-like growth factor-binding protein-3 in breast cancer cells. Relationship to transforming growth factor-beta 1 signaling. J Biol Chem 277: 7255-72561, 2002.

64. Long EM, Long MA, Tsirigotis M and Gray DA: Stimulation of the murine Uchl1 gene promoter by the B-Myb transcription factor. Lung Cancer 42: 9-21, 2003.

65. Seth P, Porter D, Lahti-Domenici J, Geng Y, Richardson A and Polyak K: Cellular and molecular targets of estrogen in normal human breast tissue. Cancer Res 62: 4540-4544, 2002.

66. Sasaki M, Honda T, Yamada H, Wake N, Barrett JC and Oshimura M: Evidence for multiple pathways to cellular senescence. Cancer Res 54: 6090-6093, 1994.

67. Forozan F, Mahlamaki EH, Monni O, Chen Y, Velman R, Jiang Y, Gooden GC, Ethier SP, Kallioniemi A and Kallioniemi OP: Comparative genomic hybridization analysis of 38 breast cancer cell lines, a basis for interpreting complementary DNA microarray data. Cancer Res 60: 4519-4525, 2000.

68. Sigal SH, Brill S, Fiorino AS and Reid LM: The liver as a stem cell and lineage system. Am J Physiol 263: G139-G148, 1992.

69. Sawyers CL, Denny CT and Witte ON: Leukemia and the disruption of normal hematopoiesis. Cell 64: 337-350, 1991.

70. Markert CL: Neoplasia: a disease of cell differentiation. Cancer Res 28: 1908-1914, 1968.